

Interference Effect in LNV and LNC Meson Decays for Left Right Symmetric Model

Rohini M. Godbole,^{1,*} Siddharth P. Maharathy,^{2,3,†} Sanjoy Mandal,^{4,‡} Manimala Mitra,^{2,3,§} and Nita Sinha^{5,3,¶}

¹Centre for High Energy Physics, Indian Institute of Science, Bengaluru - 560012, India

²Institute of Physics, Sachivalaya Marg, Bhubaneswar 751005, India

³Homi Bhabha National Institute, BARC Training School Complex, Anushakti Nagar, Mumbai 400094, India

⁴AHEP Group, Institut de Física Corpuscular, CSIC/Universitat de València, Parc Científic de Paterna. C/ Catedrático José Beltrán, 2 E-46980 Paterna (Valencia), Spain

⁵The Institute of Mathematical Sciences, C.I.T Campus, Taramani, Chennai 600 113, India

We study the effect of interference on the lepton number violating (LNV) and lepton number conserving (LNC) three-body meson decays $M_1^+ \rightarrow \ell_i^+ \ell_j^\pm \pi^\mp$, that arise in a TeV scale Left Right Symmetric model (LRSM) with nearly degenerate right handed (RH) neutrinos. LRSM contains three RH neutrinos and a RH gauge boson. The RH neutrinos of masses in the MeV-few GeV range can give resonant enhancement in the semi-leptonic LNV and LNC meson decays. In the case, where only one RH neutrino contributes to these decays, the predicted branching ratio of semi-leptonic LNV and LNC meson decays $M_1^+ \rightarrow \ell_i^+ \ell_j^+ \pi^-$ and $M_1^+ \rightarrow \ell_i^+ \ell_j^- \pi^+$ are the same. However, we find, that with at least two RH neutrinos contributing to the process, the LNV and LNC decay rates can differ. Depending on the RH neutrino mixing angles and CP violating phases, the branching ratios for the decay channels $M_1^+ \rightarrow \ell_i^+ \ell_j^+ \pi^-$ or $M_1^+ \rightarrow \ell_i^+ \ell_j^- \pi^+$ can be either enhanced or suppressed.

I. INTRODUCTION

The observation of light neutrino masses and mixings clearly indicates the existence of beyond standard model (BSM) physics. A number of models exist in the literature, that have been successful in explaining small neutrino masses and their mixings. One of the most interesting model among them is the LRSM [1], which not only explains the smallness of the light neutrino masses, but also addresses parity violation in the Standard Model (SM). The model contains three RH neutrinos, and two Higgs triplet fields, that generate the Majorana mass terms for light neutrinos via Type-I and Type-II seesaw mechanism. The RH neutrinos in this model are Majorana in nature. The Majorana masses violate lepton number and hence these neutrinos can directly induce LNV processes. The Majorana nature of the light and heavy neutrinos can be tested via lepton number violating neutrinoless double beta decay ($0\nu\beta\beta$) [2–7]. Their LNV nature can also be probed at the colliders through direct searches [8–13], as well as through the rare LNV decays of mesons and tau lep-

ton [14–25]. The $\sqrt{s} = 13$ TeV LHC search in the same-sign di-lepton and di-jet channel has so far ruled out RH neutrino masses in the $M_N \sim 100$ GeV mass range, and $M_{W_R} > 4.4$ TeV [26]. The boosted RH neutrino search for LRSM also places strong constraint on the RH gauge boson mass $M_{W_R} > 4.8$ TeV [10, 27] for the RH neutrino and RH gauge boson mass hierarchy $\mathcal{O}(0.1)$. The rare LNV and LNC semi-leptonic meson decays on the other hand are sensitive to a much smaller RH neutrino mass range $M_N \sim (\text{MeV} - \text{few GeV})$, and to a much higher value of W_R gauge boson mass. These searches are thus complementary to collider searches. It is well known that for very light and heavy neutrino masses, the rates of these LNV meson and tau decays are extremely suppressed [21, 24], well below the sensitivity reach of any future experiment. This changes dramatically, if there exists a heavy neutrino, in the MeV-GeV mass domain, which can be produced on-shell in the parent meson decay. This would lead to large resonant enhancement of these processes. Various ongoing experiments including NA62, LHCb, Belle-II are searching for the LNV meson decays. The LHCb experiment looked for the process $B^- \rightarrow \mu^- \mu^- \pi^+$, and has constrained the light neutrino-heavy neutrino mixing [15]. Due to the order of magnitude increase in the number of meson and tau flux in experiments such as SHiP, MATHUSLA and others under discussion, one expects to achieve better sensitivity for LNV meson and tau decays in future. Even non-observations can set tight limits on the rel-

* rohini@iisc.ac.in

† siddharth.m@iopb.res.in

‡ smandal@ific.uv.es

§ manimala@iopb.res.in

¶ nita@imsc.res.in

evant parameter space such as on the heavy neutrino mass M_N and RH gauge boson mass M_{W_R} [21, 28].

In this work, we study the three body LNV and LNC meson decays - $M_1^+ \rightarrow l_i^+ l_j^+ M_2^-$ and $M_1^+ \rightarrow l_i^+ l_j^- M_2^+$ for LRSM, in particular focussing on the possible interference effect in these processes, that may occur due to nearly degenerate RH neutrino states. With only a single heavy neutrino contribution, the rate of LNV and LNC meson decays are predicted to be the same, irrespective of any CP violating phase present in the RH neutrino mixing matrix. This scenario changes dramatically, if more than one heavy neutrino state contributes in these processes with non-trivial RH neutrino mixing matrix. In this case, the predictions for LNV and LNC meson decay rates can widely differ due to the interference amongst the contributions of different RH neutrinos. This leads to a change in the interpretation of data in LRSM compared to the case of single heavy neutrino. For the study of interference effect in semi-leptonic meson decays for a pure sterile neutrino without any additional gauge extension, see [25]. The interference effect in LRSM, relevant for collider searches has been discussed in [29]. The interference effects have also been studied in type-I and generalized inverse seesaw models in [30].

To quantify the interference effect in meson decays, we consider K and B -meson LNV and LNC semileptonic three body decays with a pion in the final state as illustrative examples. We develop the generic theory framework with two nearly degenerate RH neutrino states that contribute significantly in the LNV and LNC semileptonic three body meson decays. Using this we then evaluate the analytic results for the partial decay widths, and branching ratios in the presence of interference terms in the amplitude. The obtained results also hold for other semi-leptonic meson decays. We focus on the final states, that contain electrons and muons. We consider two different mass ranges of the two RH neutrino states $0.14 \text{ GeV} < M_N < 0.49 \text{ GeV}$, and $0.14 \text{ GeV} < M_N < 5 \text{ GeV}$, relevant for $K^+ \rightarrow e^+ e^\pm \pi^\mp / e^+ \mu^\pm \pi^\mp$ and $B^+ \rightarrow e^+ e^\pm \pi^\mp / e^+ \mu^\pm \pi^\mp$ meson decays, respectively. We briefly discuss the effect of interference on the future sensitivities for RH neutrino and RH gauge bosons masses in various collider and beam dump experiments.

The paper is organized as follows: In Sec. II, we first review the basic features of LRSM, following which in Sec. III we discuss in detail the RH neutrino contributions in LNV and LNC meson decays. In Sec. IV, we discuss our results with the assumption, that only two RH neutrinos are contributing with an effective 2×2 RH neutrino mixing matrix. In Sec. V, we discuss the interference effects with two RH neutrinos considering the full 3×3 RH neutrino mass mixing matrix. Fi-

nally we summarise our most important findings in the conclusions.

II. LEFT-RIGHT SYMMETRIC MODEL

LRSM is a simple extension of the Standard Model (SM), where both the left and right chiral fermions are treated on an equal footing. The model is based on the gauge group $SU(3)_c \otimes SU(2)_L \otimes SU(2)_R \otimes U(1)_{B-L}$, where the left and right chiral fermions are doublets of $SU(2)_L$ and $SU(2)_R$, respectively. The model necessarily contains three RH neutrinos (N_{Ri}) in the right-handed lepton doublet. The electric charge Q is related with third component of weak isospins I_{3L} and I_{3R} as $Q = I_{3L} + I_{3R} + (B - L)/2$. The scalar sector is also extended because of the extra symmetry. The LRSM contains one bi-doublet Φ and two scalar triplets Δ_R and Δ_L under $SU(2)_R$ and $SU(2)_L$, respectively. The particle content is given below:

$$l_L = \begin{bmatrix} \nu_{Li} \\ e_{Li} \end{bmatrix}, l_R = \begin{bmatrix} N_{Ri} \\ e_{Ri} \end{bmatrix} \quad (1)$$

$$Q_L = \begin{bmatrix} u_{Li} \\ d_{Li} \end{bmatrix}, Q_R = \begin{bmatrix} u_{Ri} \\ d_{Ri} \end{bmatrix} \quad (2)$$

$$\Phi = \begin{bmatrix} \phi_1^0 & \phi_2^+ \\ \phi_1^- & \phi_2^0 \end{bmatrix}, \Delta_{L/R} = \begin{bmatrix} \Delta_{L/R}^+/\sqrt{2} & \Delta_{L/R}^{++} \\ \Delta_{L/R}^0 & -\Delta_{L/R}^+/\sqrt{2} \end{bmatrix} \quad (3)$$

The $SU(2)$ doublets l_L and l_R have the charges $(1, 2, 1, -1)$ and $(1, 1, 2, -1)$, while the Higgs multiplets $\Phi \sim (1, 2, 2, 0)$, $\Delta_L \sim (1, 3, 1, +2)$ and $\Delta_R \sim (1, 1, 3, +2)$. The bi-doublet being neutral under $B - L$, additional Higgs triplets are required to break the left-right symmetry gauge group to the SM gauge group $SU(2) \otimes U(1)_Y$. The neutral component of Δ_R takes vacuum expectation value (VEV) v_R and breaks the gauge group $SU(2)_R \otimes U(1)_{B-L}$ to $U(1)_Y$. In the next step, VEV of bi-doublet Φ breaks the SM gauge group to $U(1)_Q$. The VEV of the bi-doublet is denoted as: $\langle \Phi \rangle = \text{Diag}(\frac{\kappa_1}{\sqrt{2}}, \frac{\kappa_2}{\sqrt{2}})$. Due to the tight constraint on ρ parameter, the VEV of Δ_L should be very small $v_L < 5 \text{ GeV}$ [31]. Hence, the different VEVs of $SU(2)$ triplets and bi-doublet follow the hierarchy $v_L \ll \kappa_{1,2} \ll v_R$. The Yukawa Lagrangian responsible for generating the lepton masses has the following form

$$-\mathcal{L}_Y = \bar{y}_L \Phi l_R + \bar{y}_L \tilde{\Phi} l_R + y_L l_L^T C^{-1} i \sigma^2 \Delta_L l_L + y_R l_R^T C^{-1} i \sigma^2 \Delta_R l_R + \text{H.C.}, \quad (4)$$

where C is the charge-conjugation operator, $C = i\gamma^2\gamma^0$ and $\tilde{\Phi} = \sigma^2\Phi^*\sigma^2$. Here γ^μ and σ^i are the Dirac and

Pauli matrices respectively, and y, \tilde{y}, y_L and y_R are the Yukawa couplings. After symmetry breaking the light and heavy neutrino mass matrix is obtained as,

$$\mathcal{M}_\nu = \begin{bmatrix} M_L & M_D \\ M_D^T & M_R \end{bmatrix} \quad (5)$$

In the above, the Dirac mass matrix $M_D = \frac{1}{\sqrt{2}}(y\kappa_1 + \tilde{y}\kappa_2) = y_D\kappa_s$, and $M_{L,R}$ are given by $M_L = \sqrt{2}v_L y_L$ and $M_R = \sqrt{2}v_R y_R$. The Higgs triplets Δ_R and Δ_L generate Majorana masses of heavy and light neutrinos. The parameter κ_s is the Electroweak VEV, and is related to $\kappa_{1,2}$ as $\kappa_s = \sqrt{\kappa_1^2 + \kappa_2^2}$. The light and heavy neutrino masses can be calculated by using the seesaw approximation $M_L \ll M_D \ll M_R$. This leads to the following light and heavy neutrino mass matrix

$$\begin{aligned} M_\nu &\sim M_L - M_D M_R^{-1} M_D^T + \mathcal{O}(M_R^{-2}) \\ &\sim \sqrt{2}v_L y_L - \frac{\kappa_s^2}{\sqrt{2}v_R} y_D f_R^{-1} y_D^T \end{aligned} \quad (6)$$

and

$$\begin{aligned} M_N &\sim M_R + \mathcal{O}(M_R^{-1}) \\ &\sim \sqrt{2}y_R v_R \end{aligned} \quad (7)$$

The mass matrix \mathcal{M}_ν in Eq. 5 can be diagonalised by a unitary transformation,

$$\mathcal{V}^T \begin{bmatrix} M_L & M_D \\ M_D^T & M_R \end{bmatrix} \mathcal{V} = \begin{bmatrix} \tilde{\mathcal{M}}_\nu & 0 \\ 0 & \tilde{\mathcal{M}}_R \end{bmatrix} \quad (8)$$

where $\tilde{\mathcal{M}}_\nu = \text{Diag}(m_1, m_2, m_3)$ and $\tilde{\mathcal{M}}_R = \text{Diag}(M_1, M_2, M_3)$. Up to $\mathcal{O}(M_R^{-2})$, the mixing matrix \mathcal{V} has the following form

$$\mathcal{V} = \begin{bmatrix} U_{\text{PMNS}} & S^\dagger \\ T & K_R^\dagger \end{bmatrix}, \quad (9)$$

where $S, T \approx M_D M_R^{-1}$. We will neglect the effect of S, T in our subsequent discussions as, $S, T \sim \mathcal{O}(10^{-5})$ for $m_\nu \sim \mathcal{O}(0.1 \text{ eV})$ and $M_N \sim \mathcal{O}(1 \text{ GeV})$.

A. Gauge Sector

In addition to the SM gauge bosons W_L and Z , this model also has RH gauge boson W_R and an additional neutral gauge boson Z' . The left and right hand gauge bosons (W_L, W_R) will mix and the mixing angle can be approximated as

$$\zeta \simeq \frac{\kappa_1 \kappa_2}{v_R^2} \simeq 2 \frac{\kappa_2}{\kappa_1} \left(\frac{M_{W_L}}{M_{W_R}} \right)^2 \quad (10)$$

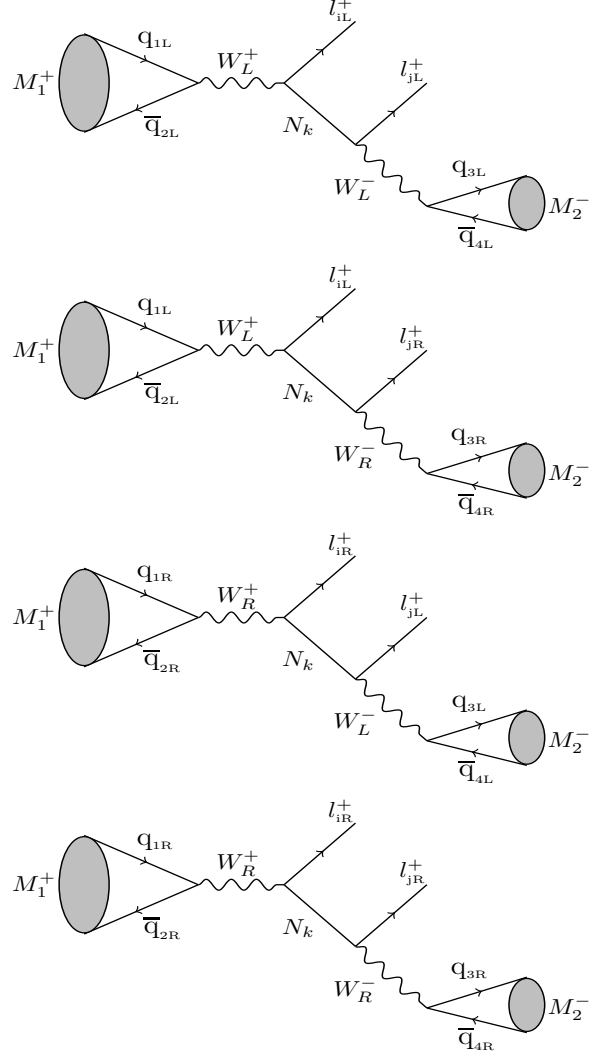


FIG. 1. The Feynman diagrams for LNV meson decays. See text for details.

Due to this small mixing between the charged gauge bosons, the masses of the gauge bosons can be approximated as

$$M_{W_L} \simeq M_{W_1} \simeq \frac{g\kappa_1}{\sqrt{2}}, \quad M_{W_R} \simeq M_{W_2} \simeq gv_R \quad (11)$$

Note that, throughout our calculation, we assume $g \equiv g_L = g_R$, which is justified, as we consider parity as a symmetry in LRSM. The mass of neutral gauge boson Z' for this choice becomes $M_{Z'} \sim 1.7M_{W_R}$.

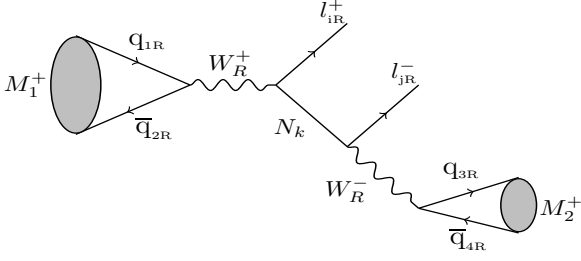


FIG. 2. The Feynman diagram for LNC meson decay.

B. Charged and neutral current Lagrangian

The charged current Lagrangian for the quark sector has the following form

$$\begin{aligned} \mathcal{L}_{cc}^q &= \frac{g}{\sqrt{2}} \sum_{i,j} \bar{u}_i V_{ij}^{\text{CKM}} W_{L\mu}^+ \gamma^\mu P_L d_j \\ &+ \frac{g}{\sqrt{2}} \sum_{i,j} \bar{u}_i V_{ij}^{\text{R-CKM}} W_{R\mu}^+ \gamma^\mu P_R d_j + \text{H.c.}, \end{aligned} \quad (12)$$

where $P_L = \frac{1}{2}(1 - \gamma_5)$ and $P_R = \frac{1}{2}(1 + \gamma_5)$. In our analysis, we consider $V^{\text{R-CKM}}$ to be the same as V^{CKM} . The charge current Lagrangian for lepton-neutrino sector is given by

$$\begin{aligned} \mathcal{L}_{CC}^l &= \frac{g}{\sqrt{2}} \sum_i \bar{l}_i W_{L\mu}^- \gamma^\mu P_L (U_{\text{PMNS}} \nu_L + S^\dagger N^c)_i \\ &+ \frac{g}{\sqrt{2}} \sum_i \bar{l}_i W_{R\mu}^- \gamma^\mu P_R (K_R^T N + T^* \nu_L^c)_i + \text{H.c.} \end{aligned} \quad (13)$$

Note that, in few of the decay channels of N_i , neutral current will also contribute. The neutral current for LRSM has the following form [32, 33]:

$$\mathcal{L}_{\text{NC}} = \frac{g}{\cos \theta_w} \left(Z_\mu J_Z^\mu + \frac{\cos^2 \theta_w}{\sqrt{\cos 2\theta_w}} Z'_\mu J_{Z'}^\mu \right) \quad (14)$$

where,

$$J_Z^\mu = \sum_i \bar{f}_i \gamma^\mu (I_{3L} P_L - Q \sin^2 \theta_w) f_i \quad (15)$$

$$J_{Z'}^\mu = \sum_i \bar{f}_i \gamma^\mu (I_{3R} P_R - \tan^2 \theta_w (Q - I_{3L})) f_i. \quad (16)$$

As emphasized before, for the particular choice of the neutrino mixing matrix \mathcal{V} , we neglect interaction terms proportional to the mixing matrices S and T . Note that, masses of both the RH gauge bosons and RH neutrinos are proportional to $SU(2)_R$ breaking scale v_R . However, since the RH neutrino masses also depend on the Yukawa couplings of Δ_R with the heavy neutrinos,

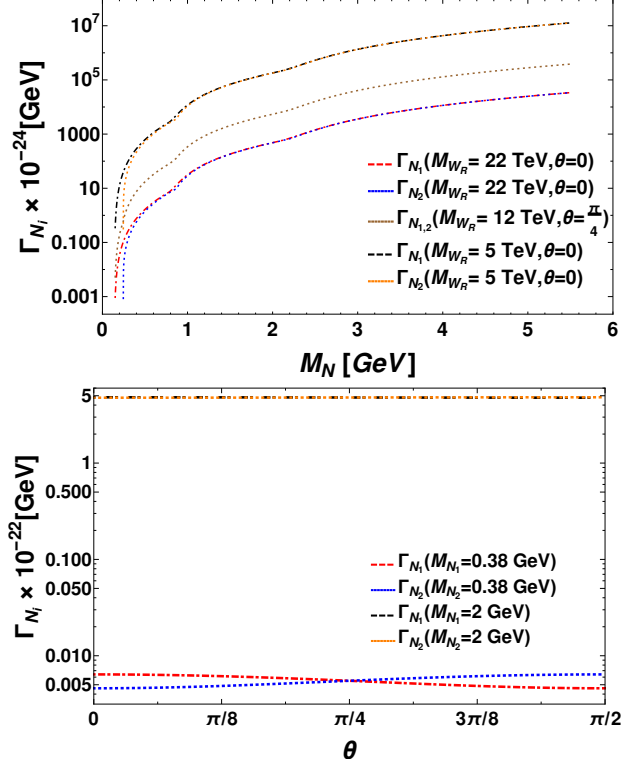


FIG. 3. Upper panel: variation of the decay widths of the RH neutrino states $N_{1,2}$ with the masses of RH neutrinos for different values of θ and RH gauge boson mass M_{W_R} . Lower panel: variation of the decay widths of $N_{1,2}$ with θ . For $M_{N_{1,2}} = (0.38, 2)$ GeV, we consider $M_{W_R} = (22, 5)$ TeV, respectively.

one can choose to have a wide splitting between the two. In this paper we consider the masses of the heavy neutrino in the MeV-GeV range, in particular, in between $0.14 \text{ GeV} < M_{N_i} < 5 \text{ GeV}$, so that the decay of the mesons can produce on-shell RH neutrinos. Semileptonic meson decays, such as $M_1^+ \rightarrow l_i^+ l_j^\pm M_2^\mp$ will be then resonantly enhanced due to the on-shell production of the RH neutrinos.

III. LNV AND LNC MESON DECAYS

Lepton number is not conserved in LRSM as the massive neutrinos are Majorana particles. The heavy neutrino being Majorana particles, can result in LNV as well as LNC meson decay processes:

$$\text{LNV} : M_1^+(p) \rightarrow l_i^+(k_1) + l_j^+(k_2) + M_2^-(k_3) \quad (17)$$

$$\text{LNC} : M_1^+(p) \rightarrow l_i^+(k_1) + l_j^-(k_2) + M_2^+(k_3), \quad (18)$$

In the above, M_1 is a pseudoscalar meson and M_2 can be either a pseudoscalar or a vector meson. In this work, we consider only the case of pseudoscalar M_2 . We assume, that there are atleast two RH neutrinos with masses in between 100 MeV–5 GeV range, that mediate these meson decays. The Feynman diagrams for the LNV process are shown in Fig. 1. The different contributions are mediated through $W_L - N_k - W_L$, $W_L - N_k - W_R$, $W_R - N_k - W_L$ and $W_R - N_k - W_R$, respectively. Note that, while $W_R - N_k - W_R$ diagram completely depends on the mixing matrix in the RH neutrino sector, the other diagrams also depend on the light-heavy neutrino mixing. Throughout this work, we consider the contribution from $W_R - N_k - W_R$ diagram only, as the light-heavy neutrino mixing angle which comes from the off-diagonal blocks (S, T) of mixing matrix \mathcal{V} is very small. Considering the heavy neutrinos to be $\mathcal{O}(\text{MeV})$, the RH neutrinos can be produced on-shell and the semi-leptonic meson decay will be resonantly enhanced. In addition, there can also be contribution from $W_L - W_R$ mixing in one of the legs, but these are suppressed due to small mixing angle ζ . The contributions from the light neutrino mediated process will be much smaller due to the mass-suppression. Hence we do not consider all of these other contributions in our analysis. In Fig. 2, we have shown the Feynman diagram for LNC process.

The contribution from heavy neutrinos N_a to the

decay amplitude of the LNV process $M_1^+(p) \rightarrow l_i^+(k_1)l_j^+(k_2)M_2^-(k_3)$ can be written as,

$$\mathcal{M}_{ij}^{\text{LNV},a} = (\mathcal{M}_{\text{lep}}^{\mu\nu})_a^i \mathcal{M}_{\mu\nu}^{\text{had}} \quad (19)$$

where

$$\begin{aligned} \mathcal{M}_{\mu\nu}^{\text{had}} &= \frac{G_F}{\sqrt{2}} M_{W_L}^2 V_{M_1}^{\text{CKM}} V_{M_2}^{\text{CKM}} \langle 0 | \bar{q}_2 \gamma_\mu \gamma^5 q_1 | M_1^+(p) \rangle \\ &\langle M_2^-(k_3) | \bar{q}_3 \gamma_\nu \gamma^5 | 0 \rangle \\ &= \frac{G_F}{\sqrt{2}} M_{W_L}^2 V_{M_1}^{\text{CKM}} V_{M_2}^{\text{CKM}} f_{M_1} f_{M_2} p_\mu k_{3\nu}. \end{aligned} \quad (20)$$

In the above, G_F is the Fermi coupling constant, $V_{M_1}^{\text{CKM}}$, $V_{M_2}^{\text{CKM}}$ are the Cabbibo-Kobayashi-Maskawa (CKM) matrix elements at the annihilation (creation) vertex of the meson $M_1(M_2)$, f_{M_1} , f_{M_2} are the decay constant of M_1 , M_2 . The relevant leptonic matrix element for ($\Delta L=2$) LNV process is given by the following product of two charged currents

$$\begin{aligned} \mathcal{M}_{\text{lep}}^{\mu\nu} &\propto (\bar{N} \gamma^\mu P_R l) (\bar{N} \gamma^\nu P_R l) \\ &= (\bar{N}_a (K_R^*)_{ai} \gamma^\mu P_R l_i) (\bar{N}_a (K_R^*)_{aj} \gamma^\nu P_R l_j) \\ &= (\bar{l}_i^c K_{Rai}^* \gamma^\mu P_L N_a) (\bar{N}_a K_{Raj}^* \gamma^\nu P_R l_j), \end{aligned} \quad (21)$$

where we have used the fact that massive neutrinos are Majorana type ($N_a^c = N_a$). We can now write the leptonic part of the amplitude as

$$(\mathcal{M}_{\text{lep}}^{\mu\nu})_a^i = 2\sqrt{2}G_F \frac{M_{W_L}^2}{M_{W_R}^4} (K_R^*)_{ai} (K_R^*)_{aj} M_{N_a} \frac{\bar{u}(k_1) \not{p} \not{k}_3 P_R v(k_2)}{q^2 - M_{N_a}^2 + i\Gamma_{N_a} M_{N_a}}, \quad (22)$$

where $q = p - k_1$. The $1/M_{W_R}^4$ term appears due to the two W_R gauge boson propagators in the lower-most

panel of Fig. 1. Finally, we can write the individual contribution from heavy neutrino N_a to the amplitude as

$$\mathcal{M}_{ij}^{\text{LNV},a} = 2G_F^2 V_{M_1}^{\text{CKM}} V_{M_2}^{\text{CKM}} f_{M_1} f_{M_2} \left(\frac{M_{W_L}}{M_{W_R}} \right)^4 (K_R^*)_{ai} (K_R^*)_{aj} M_{N_a} \frac{\bar{u}(k_1) \not{p} \not{k}_3 P_R v(k_2)}{q^2 - M_{N_a}^2 + i\Gamma_{N_a} M_{N_a}}, \quad (23)$$

where Γ_{N_a} is the decay width of heavy neutrino N_a , obtained by summing over all accessible final states. Adding the contributions from all heavy neutrinos, we

can write the full amplitude as

$$\mathcal{M}^{\text{LNV}} = \sum_{a=1}^3 \left(\mathcal{M}_{ij}^{\text{LNV},a} + \mathcal{M}_{ji}^{\text{LNV},a} \right) \quad (24)$$

where the second contribution is coming from the ex-

change of two leptons. Finally the total amplitude square, $|\mathcal{M}^{\text{LNV}}|^2$ can be written as

$$|\mathcal{M}^{\text{LNV}}|^2 = \sum_{a,b=1; b>a}^3 \left(|\mathcal{M}_{ij}^{\text{LNV},a}|^2 + |\mathcal{M}_{ji}^{\text{LNV},a}|^2 + 2\text{Re} \left[(\mathcal{M}_{ij}^{\text{LNV},a})^\dagger (\mathcal{M}_{ij}^{\text{LNV},b}) \right] + 2\text{Re} \left[(\mathcal{M}_{ji}^{\text{LNV},a})^\dagger (\mathcal{M}_{ji}^{\text{LNV},b}) \right] \right) \quad (25)$$

The explicit form of these squared matrix elements are provided in the Appendix A. The RH neutrino state N_i of mass MeV to few GeV can decay to various final states, such as, $l^\pm V^\mp, l^\pm P^\mp, \nu_l V^0, \nu_l P^0$, where V, P are the vector, and pseudoscalar mesons. We show the decay width of the RH neutrino state $N_{1,2}$ in Fig. 3, following the parametrization given in Eq. 32. The upper panel represents the variation of the decay widths of $N_{1,2}$ with the masses of the RH neutrinos, and lower panel represents the variation w.r.t θ . We find that, for smaller values of $M_{N_{1,2}}$, the dependency of decay

width on mixing angles are more prominent, whereas for higher values of $M_{N_{1,2}}$, the θ dependency is negligible. This is clearly evident from the lower panel, where for $M_N = 2$ GeV, both the decay widths $\Gamma_{N_{1,2}}$ co-inside. In the upper panel, that represents decay widths for various θ , the decay widths of $N_{1,2}$ show some difference for smaller masses, and for $\theta \neq \pi/4$, while for larger masses $M_{N_{1,2}} > 1.5$ GeV, both the decay widths become same. This will have an impact on the estimated branching ratios for K and B mesons, which we will discuss in the subsequent sections. From Fig. 3, it is evident, that the decay width of RH neutrino is indeed very small for our chosen mass range. Hence, we can safely use the narrow width approximation,

$$|\mathcal{M}_{ij}^{\text{LNV},a}|^2 \propto \frac{1}{((p-k_1)^2 - M_{N_a}^2)^2 + \Gamma_{N_a}^2 M_{N_a}^2} = \frac{\pi}{M_{N_a} \Gamma_{N_a}} \delta((p-k_1)^2 - M_{N_a}^2) \quad (26)$$

Note that, we are neglecting terms like $(\mathcal{M}_{ij}^{\text{LNV},a})^\dagger \mathcal{M}_{ji}^{\text{LNV},b}$ as

$$(\mathcal{M}_{ij}^{\text{LNV},a})^\dagger \mathcal{M}_{ji}^{\text{LNV},b} \propto \frac{1}{\left((p-k_1)^2 - M_{N_a}^2 - i\Gamma_{N_a} M_{N_a} \right) \left((p-k_2)^2 - M_{N_b}^2 + i\Gamma_{N_b} M_{N_b} \right)} \neq \frac{\pi}{M_{N_a} \Gamma_{N_a}} \delta((p-k_1)^2 - M_{N_a}^2) \quad (27)$$

Hence, contributions from these terms will not be resonantly enhanced and can be safely neglected compared to other terms, see Ref. [24]. Finally, the LNV decay rate can be written as

$$d\Gamma^{\text{LNV}} = \left(1 - \frac{\delta_{ij}}{2} \right) \frac{1}{2m} |\mathcal{M}^{\text{LNV}}|^2 d_3(\text{PS}; p \rightarrow k_1 k_2 k_3) \quad (28)$$

where $d_3(\text{PS}; p \rightarrow k_1 k_2 k_3)$ is the three-body phase space which can be written in terms of product of two two-

body phase space as follows

$$d_3(\text{PS}; p \rightarrow k_1 k_2 k_3) = d_2(\text{PS}; p \rightarrow k_1 q) dq^2 d_2(\text{PS}; q \rightarrow k_2 k_3) \quad (29)$$

The full analytical expression for the LNV decay width and three-body phase space are given in Appendix. A. Similarly the LNC process can also be mediated by the heavy neutrinos via the following leptonic part of matrix element:

$$\mathcal{M}_{\text{lep}}^{\mu\nu} \propto (\bar{l} \gamma^\mu P_R N) (\bar{N} \gamma^\nu P_R l) = (\bar{l}_i \gamma^\mu P_R (K_R^T)_{ia} N_a) (\bar{N}_a (K_R^*)_{aj} \gamma^\nu P_R l_j) \quad (30)$$

and the amplitude coming from individual contribution

of heavy neutrino N_a is given by

$$\mathcal{M}_{ij}^{\text{LNC},a} = 2G_F^2 V_{M_1}^{\text{CKM}} V_{M_2}^{\text{CKM}} f_{M_1} f_{M_2} \left(\frac{M_{WL}}{M_{WR}} \right)^4 (K_R)_{ai} (K_R^*)_{aj} \frac{\bar{u}(k_1) \not{p} \not{q} k_3' P_R v(k_2)}{q^2 - M_{N_a}^2 + i\Gamma_{N_a} M_{N_a}} \quad (31)$$

Following the same approach as LNV case, one can also derive the partial decay width for LNC process. The details are given in Appendix. A. In the subsequent sections, we will consider a simplified scenario, where both the RH neutrino states $N_{1,2}$ can give resonantly enhanced contributions in the LNV and LNC processes, and we will quantify the effect of the interference.

Note that, the RH neutrinos of mass MeV – few GeV can also be constrained from cosmological constraints. A RH neutrino with a mixing angle θ with the active neutrino, can decay to leptonic and hadronic final states. If the decay happens around the time of Big Bang Nucleosynthesis (BBN) $\tau \gtrsim 1$ sec, this can alter the prediction of light element abundance in the Universe. Constraints from BBN on the MeV scale RH neutrino have been discussed in detail in [34], with the assumption of a pure sterile neutrino. Also, see [35, 36] for a generic discussion on BBN constraints for a late decaying massive state X . Similar constraints would also be applicable for LRSM, where the RH neutrino decays via off-shell W_R gauge bosons, and lead to semi-leptonic final states. We estimate the lifetime of the RH neutrino states for 380 MeV and 2 GeV, and the RH gauge boson masses as 5 TeV, and 22 TeV. We find that, the RH neutrino lifetime varies in $10^{-6} - 1$ sec. For these RH neutrino masses, that are optimistic for semi-leptonic kaon and B meson decays, a heavier RH gauge boson of mass more than 22 TeV will therefore be tightly constrained from BBN. Note that, the decay width/lifetime of the RH neutrino states can be made larger/smaller, if additional channels for RH neutrino decay open up. For, example, with a sizeable active-sterile mixing S, T in Eq. 13, the decay lifetime can be made sufficiently smaller, and hence BBN constraints can be avoided. In that scenario, additional diagrams $L - R, L - L$ shown in Fig. 1 will also contribute in three body LNV and LNC meson decays. The detail evaluation of these processes is beyond the scope of this paper, and will be pursued elsewhere.

IV. ANALYSIS FOR THE CASE OF TWO GENERATIONS

We consider that two of the heavy neutrino states are nearly degenerate i.e. $M_{N_1} \sim M_{N_2}$ and M_{N_3} to be very heavy. The two degenerate states mediate the LNV and LNC meson decays of K , and B mesons, and give resonance enhancement in the branching ratios. The

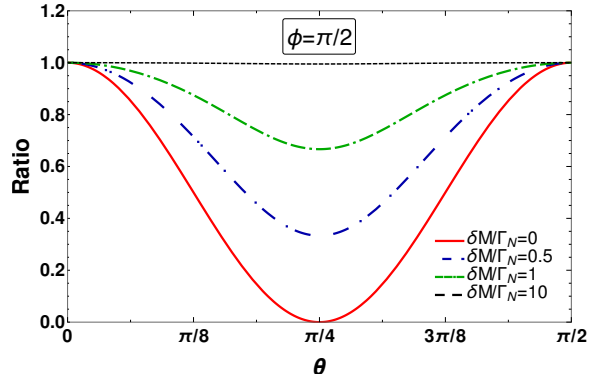


FIG. 4. Variation of the ratio of LNV and LNC branching ratios of $K^+ \rightarrow l^+ l^\pm \pi^\mp$ with the mixing angle θ . The red solid, blue dashed-double-dotted, green dashed-dotted, and black dashed lines represent four different $\delta M/\Gamma$ ratios (0,0.5,1,10). The RH neutrino mass has been set at $M_N \sim 0.38$ GeV.

choice of the RH neutrino masses can be justified, as we have free parameters y_D and y_R in the Lagrangian Eq. 4, that can be adjusted to give eV light neutrino mass, along with two nearly degenerate RH neutrinos. The matrix K_R is in general a 3×3 unitary matrix with few angles, and phases. However, to present the effect of interference in a simplified way, we choose the following parameterisation of K_R ,

$$K_R = \begin{bmatrix} \cos \theta & \sin \theta & 0 \\ -e^{i\phi} \sin \theta & e^{i\phi} \cos \theta & 0 \\ 0 & 0 & 1 \end{bmatrix}, \quad (32)$$

The above matrix K_R is just the product of one orthogonal matrix with angle θ , and a diagonal phase matrix. By the choice of such parameterisation, we are looking only at mixing between the two flavours (N_1, N_2) which have been assumed to have degenerate or nearly degenerate masses. The parameterisation of the mixing matrix K_R enables the decay of meson into e , and μ lepton flavors, and restricts final states with any taus. In the subsequent section, we explicitly demonstrate the impact of this angle and phase on LNV and LNC meson decay rates.

Note that, in addition to the mixing angle, and phase, the contributions of N_1 and N_2 states in LNV and LNC decays also depend on the mass difference of the RH neutrino states $N_{1,2}$, as well as their decay widths. For degenerate or almost nearly degenerate masses of RH

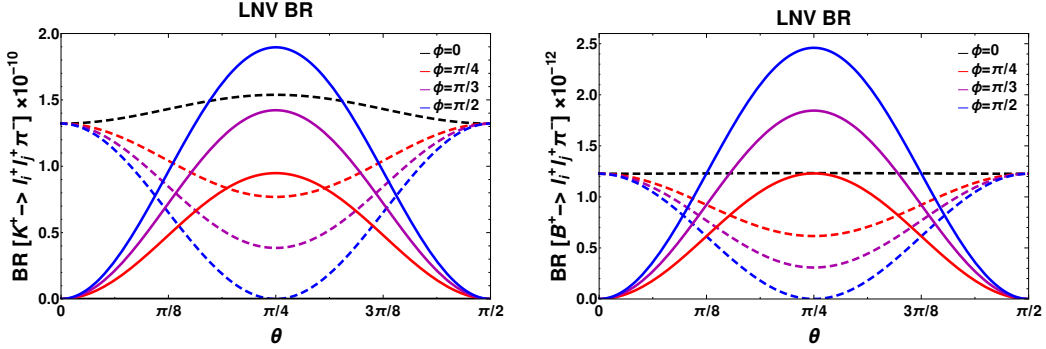


FIG. 5. Branching ratio of LNV meson decay to same flavour (e^+, e^+) and different flavour (e^+, μ^+) final state along with a pion (π^+). The plot in the left panel is for kaon (K^+), and the plot in the right panel is for B-meson (B^+) decay, respectively. The BR is not constant rather shows constructive and destructive interference effect for different values of θ and ϕ . The dotted line and solid line correspond to e^+e^+ and $e^+\mu^+$ mode respectively. For K^+ decay we have considered $M_N \simeq 0.38$ GeV and $M_{W_R} = 22$ TeV, and for B^+ -meson decay we have considered $M_N \simeq 2$ GeV and $M_{W_R} = 5$ TeV, respectively.

neutrinos, the states $N_{1,2}$ will both be resonantly produced in the K, B meson decays. Depending upon the angle and phases of the mixing matrix, the contribution of the $N_{1,2}$ states can either interfere constructively or destructively. However, for a very large mass difference between the $N_{1,2}$ states, the interference effect would fade away. Therefore, the LNV and LNC meson decays for a large mass splitting between the RH neutrinos is similar to the one generation case, that has been studied in detail in [14, 19, 21, 24]. To demonstrate the effect of the mass splitting δM , and the decay width $\Gamma = \frac{\Gamma_{N_1} + \Gamma_{N_2}}{2}$ on the interference effect, in Fig. 4, we show the ratio of LNV and LNC branching ratios for different values of the $\delta M/\Gamma$. The ratio of mass difference between two states $N_{1,2}$ and the decay width Γ has a large impact on the interference effect. Without any interference effect, the LNV and LNC branching ratio would be same, leading to the ratio to be identity. For a very small value of $\delta M/\Gamma$, the ratio deviates significantly from identity. As is evident from the figure, increasing $\delta M/\Gamma$ ratio, the interference between $N_{1,2}$ state tends to become less prominent, and for large value, the interference effect and the oscillatory behaviour fade away, leading to the LNV and LNC branching ratios to be equal.

A. LNV

We give the complete list of decay channels of N_i for general light-heavy mixing matrix in Appendix B. We list only the channels that will contribute for RH neutrino masses in the range $0.14 \text{ GeV} < M_{N_i} < 5 \text{ GeV}$. Note that, for our chosen mass range of RH neu-

trino states and with the off-diagonal mixing elements $S, T \sim 0$, decay modes such as $N \rightarrow l^\pm P^\mp, l^\pm V^\pm, \nu_l P^0$ and $\nu_l V^0$ will only contribute. With the mixing matrix K_R given in Eq. 32, RH neutrino decay width will also depends on the mixing angle θ . One can write down a generic expression for the total decay width of degenerate RH neutrinos as,

$$\Gamma_{N_1} = \frac{1}{M_{W_R}^4} \left(A(M_N) + B(M_N) \cos 2\theta \right), \quad (33)$$

$$\Gamma_{N_2} = \frac{1}{M_{W_R}^4} \left(A(M_N) - B(M_N) \cos 2\theta \right) \quad (34)$$

Note that, these above expressions can be obtained by substituting K_R into the expressions of the decay widths given in the Appendix B, where we considered $S, T \sim 0$. For the choice of $M_{N_1} \sim M_{N_2} \sim M_N = 0.38$ GeV, that we consider for K^+ meson decay, the RH neutrinos will have only a fewer decay modes with a charged pion in the final state, i.e. $N_j \rightarrow l_i^\pm + \pi^\mp$. The expressions of the two functions, $A(M_N)$ and $B(M_N)$ have a simpler form, and have been given in the Appendix B (see Eq. B2 and Eq. B3). We note that, for relatively larger mass $M_{N_i} > 1.5$ GeV of the RH neutrino states, decay widths are independent of the mixing angle θ . This can be understood easily as follows. We can neglect the final state lepton masses in evaluating the decay widths for few GeV RH neutrino masses. The unitarity relation for the mixing matrix K_R leads the total decay widths of $N_{1,2}$ independent of θ . In this case, one can write down the expression for the total decay width as

$$\Gamma_{N_1} = \frac{1}{M_{W_R}^4} A(M_{N_1}), \quad \Gamma_{N_2} = \frac{1}{M_{W_R}^4} A(M_{N_2}). \quad (35)$$

Here $A(M_N)$ is function of the mass M_N , and can be derived from different decay modes, given in the Appendix B. Therefore, for degenerate masses ($M_{N_1} = M_{N_2} \equiv M_N$), the above two decay widths will be the same. We further find that, LNV partial width for the parent meson M_1 has the following dependencies upon

the mixing angle and phase

$$\Gamma^{\text{LNV}} \propto \begin{cases} (1 - \sin^2 2\theta \sin^2 \phi), & \text{for } i = j \\ (\sin^2 2\theta \sin^2 \phi), & \text{for } i \neq j \end{cases} \quad (36)$$

which is consistent with the Ref. [29]. In the above equation i, j can either be e or μ .

Using this general form of the N decay width given in Eq. 33 and Eq. 34, one can write down the LNV decay rate of the parent meson M_1 into same flavour leptons and it leads to a rather complicated expression. The explicit expressions for the ee and $\mu\mu$ case are as follows:

$$\Gamma_{ee}^{\text{LNV}} = \beta \left(\frac{\cos^4 \theta}{A(M_N) + B(M_N) \cos 2\theta} + \frac{\sin^4 \theta}{A(M_N) - B(M_N) \cos 2\theta} + \frac{1}{4} \cos 2\phi \sin^2 2\theta \right. \\ \left. \left[\frac{1}{A(M_N) + B(M_N) \cos 2\theta} + \frac{1}{A(M_N) - B(M_N) \cos 2\theta} \right] \right) f^{ee}(M_N) \quad (37)$$

$$\Gamma_{\mu\mu}^{\text{LNV}} = \beta \left(\frac{\sin^4 \theta}{A(M_N) + B(M_N) \cos 2\theta} + \frac{\cos^4 \theta}{A(M_N) - B(M_N) \cos 2\theta} + \frac{1}{4} \cos 2\phi \sin^2 2\theta \right. \\ \left. \left[\frac{1}{A(M_N) + B(M_N) \cos 2\theta} + \frac{1}{A(M_N) - B(M_N) \cos 2\theta} \right] \right) f^{\mu\mu}(M_N) \quad (38)$$

The partial decay width for different outgoing flavours

is given by

$$\Gamma_{e\mu}^{\text{LNV}} = \beta \left(\frac{\sin^2 2\theta}{4(A(M_N) + B(M_N) \cos 2\theta)} + \frac{\cos^2 2\theta}{4(A(M_N) - B(M_N) \cos 2\theta)} - \frac{1}{4} \cos 2\phi \sin^2 2\theta \right. \\ \left. \left[\frac{1}{A(M_N) + B(M_N) \cos 2\theta} + \frac{1}{A(M_N) - B(M_N) \cos 2\theta} \right] \right) f^{e\mu}(M_N) \quad (39)$$

where $\beta = \frac{1}{128\pi^3} \frac{M_{WL}^8}{M_{WR}^4} G_F^2 (V_{M_1}^{\text{CKM}} V_{M_2}^{\text{CKM}})^2 f_{M_1}^2 f_{M_2}^2$. The functions f^{ee} , $f^{\mu\mu}$ and $f^{e\mu}$ can be identified from the Eq. A10. The first two terms are due to the individual $N_{1,2}$ contributions in the decay amplitude. The term in the partial decay width expressions proportional to $\cos 2\phi \sin^2 2\theta$ is due to the interference of the $N_{1,2}$ contributions.

The branching ratios of the different LNV modes of

the parent meson M_1 are then given by

$$\text{Br}(M_1^+ \rightarrow l_i^+ l_j^+ M_2^-) = \frac{\Gamma_{ij}^{\text{LNV}}}{\Gamma_{M_1^+}} \quad (40)$$

where $\Gamma_{M_1^+}$ is the total decay width of the parent meson. In Fig. 5, we show the branching ratios of LNV meson decay $K^+/B^+ \rightarrow e^+e^+\pi^-$, and $K^+/B^+ \rightarrow e^+\mu^+\pi^-$ vs mixing angle θ for different values of ϕ . The left panel corresponds to the kaon decay. We consider the

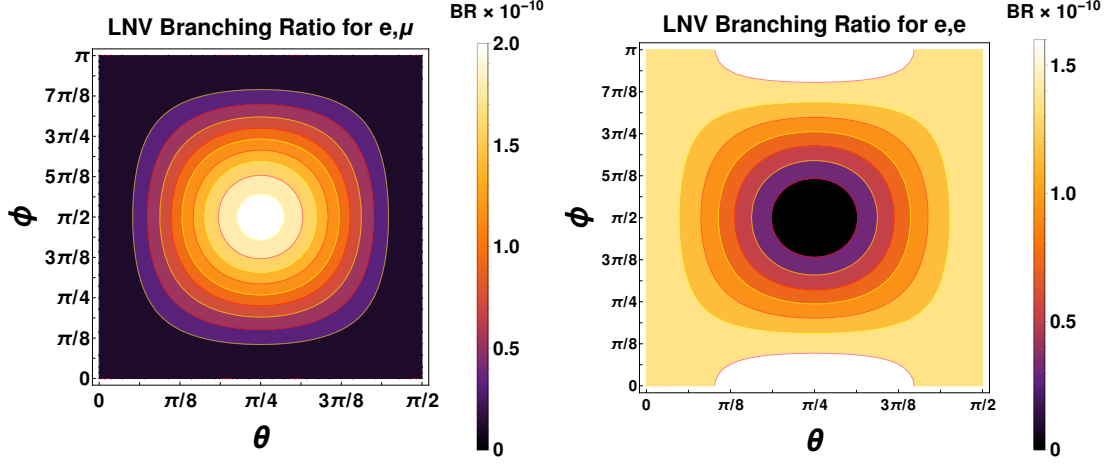


FIG. 6. Left panel: variation of the branching ratio of LNV kaon decay $K^+ \rightarrow e^+ \mu^+ \pi^-$ with the variation of the angle and phase (θ, ϕ). The final states leptons are of same charge, and different flavours. Right panel: the same, however for final states with same charge and same lepton flavours $K^+ \rightarrow e^+ e^+ \pi^-$. The masses of RH neutrino and RH gauge bosons are $M_{W_R} = 22$ TeV and $M_{N_1} \simeq M_{N_2} \simeq 0.38$ GeV. The maximum value of the branching ratios are at $\mathcal{O}(10^{-10})$, consistent with the present experimental bounds

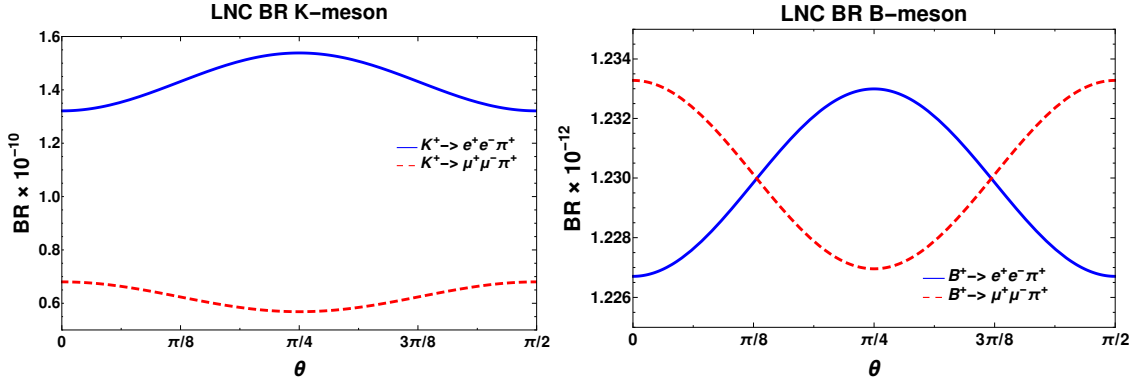


FIG. 7. Variation of LNC branching ratio of K^+ meson and B^+ meson decay to same flavour (e^+, e^-) and (μ^+, μ^-) final state leptons with the mixing angle θ . For K^+ decay we have considered $M_N \simeq 0.38$ GeV and $M_{W_R} = 22$ TeV, and for B^+ meson decay we have considered $M_N \simeq 2$ GeV and $M_{W_R} = 5$ TeV, respectively.

mass of the RH gauge boson as $M_{W_R} = 22$ TeV ¹, and mass of heavy neutrino as $M_N \simeq 0.38$ GeV. The

¹ Note that, for K^+ meson, and B^+ meson decay, we consider the mass of the RH gauge boson as 22 TeV and 5 TeV, and the RH neutrino masses as 0.38 GeV, and 2 GeV, respectively. For these benchmark points, the branching ratios are consistent with the experimental limits. The chosen RH neutrino benchmark mass point $M_N = 2$ GeV, for which we consider a 5 TeV M_{W_R} is unconstrained from K^+ meson decays. A different value of the RH gauge boson mass will simply give an overall scaling in the branching ratios and will not change the nature

of Fig. 5 any way. This holds true for other figures, relevant for LNC modes. MeV order neutrino mass is responsible for the on-shell production of RH neutrinos. In the right panel, we show the LNV decay of B^+ meson. For this case, we consider the RH gauge boson mass to be $M_{W_R} = 5$ TeV, and mass of heavy neutrino is $M_N \simeq 2$ GeV. The branching ratios derived for these benchmark mass points are consistent with the experimental limits $\text{Br}(K^+ \rightarrow e^+ e^+ \pi^-, e^+ \mu^+ \pi^-) < (6.4, 5.0) \times 10^{-10}$ and

of Fig. 5 any way. This holds true for other figures, relevant for LNC modes.

$\text{Br}(B^+ \rightarrow e^+e^+\pi^-, e^+\mu^+\pi^-) < (2.3, 15.0) \times 10^{-8}$, respectively [37]. The figures confirm the angular dependencies of the branching ratios of LNV decay process. The solid and dashed lines correspond to $e^+\mu^+$, and e^+e^+ channels. Note that, the e^+e^+ and $e^+\mu^+$ channels have complimentary nature w.r.t the angular variables. This can further be highlighted by a contour plot in the θ - ϕ plane. Fig. 6 shows the variation of LNV branching ratios of $K^+ \rightarrow e^+e^+\pi^-$, and $K^+ \rightarrow e^+\mu^+\pi^-$ processes for different values of mixing angle θ and phase ϕ . With two degenerate heavy neutrinos, the branching ratio of the above processes exhibit constructive and destructive interferences, as is clearly evident from the figures. The white region in the right panel of Fig. 6, occurs as for

$\theta = \pi/4$, and $\phi = 0$, the LNV branching ratio to e^+e^+ channel shows a maxima (see left panel of Fig. 5). For B^+ meson, the plots are very similar. Hence, we do not show them explicitly.

B. LNC

The parent meson can decay via LNC processes $M_1^+ \rightarrow l_i^+ l_j^- M_2^+$. The RH neutrino states $N_{1,2}$ will mediate these processes. Considering the general form of N_i decay width as given in Eq. 34, LNC decay rate will be modified. For ee and $\mu\mu$ channel the decay rate is given by

$$\Gamma_{ee}^{\text{LNC}} = \beta \left(\frac{\cos^4 \theta}{A(M_N) + B(M_N) \cos 2\theta} + \frac{\sin^4 \theta}{A(M_N) - B(M_N) \cos 2\theta} + \frac{1}{4} \sin^2 2\theta \right) \left[\frac{1}{A(M_N) + B(M_N) \cos 2\theta} + \frac{1}{A(M_N) - B(M_N) \cos 2\theta} \right] h^{ee}(M_N) \quad (41)$$

$$\Gamma_{\mu\mu}^{\text{LNC}} = \beta \left(\frac{\sin^4 \theta}{A(M_N) + B(M_N) \cos 2\theta} + \frac{\cos^4 \theta}{A(M_N) - B(M_N) \cos 2\theta} + \frac{1}{4} \sin^2 2\theta \right) \left[\frac{1}{A(M_N) + B(M_N) \cos 2\theta} + \frac{1}{A(M_N) - B(M_N) \cos 2\theta} \right] h^{\mu\mu}(M_N) \quad (42)$$

and for $e\mu$ channel, the decay rate has the following

form,

$$\Gamma_{e\mu}^{\text{LNC}} = \beta \left(\frac{\sin^2 2\theta}{4(A(M_N) + B(M_N) \cos 2\theta)} + \frac{\sin^2 2\theta}{4(A(M_N) - B(M_N) \cos 2\theta)} - \frac{1}{4} \sin^2 2\theta \right) \left[\frac{1}{A(M_N) + B(M_N) \cos 2\theta} + \frac{1}{A(M_N) - B(M_N) \cos 2\theta} \right] h^{e\mu}(M_N) \quad (43)$$

The functions h^{ee} , $h^{\mu\mu}$ and $h^{e\mu}$ can be identified from Eq. A14. We find that, for different lepton flavors, and for degenerate RH neutrino mediators $M_{N_1} = M_{N_2} = M_N > 1.5$ GeV, LNC partial decay width becomes zero, as $B(M_N) = 0$. This occurs for the LNC decay mode of B^+ meson $B^+ \rightarrow e^+\mu^-\pi^+$. On the contrary, for same flavoured leptons, the partial width is

independent of the mixing angle θ [29]. For the K^+ meson, the preferred mass range of the RH neutrino states are $0.14 \text{ GeV} < M_N < 0.49 \text{ GeV}$. The total decay width of the mediators $N_{1,2}$ has a θ dependency in this mass range. The partial decay width of the process $K^+ \rightarrow e^\pm \mu^\mp \pi^+$, is therefore non-zero. This leads to a very small LNC branching ratio $\mathcal{O}(10^{-15})$

which is beyond the sensitivity reach of future experiments. We therefore do not explicitly show the results for the LNC $e\mu$ case. Fig. 7 represents the variation of the branching ratios of the LNC decay modes $K^+/B^+ \rightarrow e^+e^-\pi^+/\mu^+\mu^-\pi^+$. Note that, there is no dependency on the phase ϕ . For the $K^+ \rightarrow e^+e^-\pi^+$ mode, the branching ratio is very similar as the LNV mode $K^+ \rightarrow e^+e^+\pi^-$ with $\phi = 0$ (see Fig. 5). The qualitative nature of the LNC branching ratios can be understood from Eq. 42 and Eq. 43. For a constant heavy neutrino decay width Γ_N the LNC decay width should have constant value, but the oscillatory behaviour is due to the fact that the heavy neutrino decay width also depends on mixing angle θ . Finally, we show the ratio of the LNV and LNC decay of K^+ and B^+ -meson for ee final state in Fig. 8. In the absence of any interference, the ratio would have been identity. The deviation from unity occurs due to the relative enhancement/suppression of the LNV and LNC branching ratio because of the presence of interference terms.

In order to discuss the impact of the CP phase and mixing angle on the LNV or LNC decay widths, we further define the following two asymmetries R and \tilde{R} as,

$$R = \frac{\Gamma_{K^+ \rightarrow e^+e^-\pi^+}^{\text{LNC}} - \Gamma_{K^+ \rightarrow e^+e^+\pi^-}^{\text{LNV}}}{\Gamma_{K^+ \rightarrow e^+e^-\pi^+}^{\text{LNC}} + \Gamma_{K^+ \rightarrow e^+e^+\pi^-}^{\text{LNV}}} \quad (44)$$

$$\tilde{R} = \frac{\Gamma_{K^+ \rightarrow e^+e^+\pi^-}^{\text{LNV}} - \Gamma_{K^+ \rightarrow e^+\mu^+\pi^-}^{\text{LNV}}}{\Gamma_{K^+ \rightarrow e^+e^+\pi^-}^{\text{LNV}} + \Gamma_{K^+ \rightarrow e^+\mu^+\pi^-}^{\text{LNV}}} \quad (45)$$

Fig. 9 shows the variation of R (left panel) and \tilde{R} (right panel) for different values of the mixing angle θ and phase ϕ . It is evident from this figure that R and \tilde{R} varies between $[0 : 1]$ and $[-1 : 1]$, respectively. Note that R and $|\tilde{R}|$ have complimentary nature w.r.t the angular variables. Hence simultaneous measurements of R and \tilde{R} can shed some light on the values of θ and ϕ . Similar results can also be obtained from B decays.

In Fig. 10, we represent the effect of interference in the $M_N - M_{W_R}$ mass plane. We consider two different decay modes $K^+/B^+ \rightarrow e^+\mu^+\pi^-$, and $K^+/B^+ \rightarrow e^+e^+\pi^-$. The solid red line in the left panel has been derived by assuming only one generation RH neutrino state N_1 . This corresponds to the present experimental limit of the branching ratio $K^+ \rightarrow e^+\mu^+\pi^-$, which is $\text{Br}(K^+ \rightarrow e^+\mu^+\pi^-) < 5 \times 10^{-10}$ [37]. The blue dashed and blue solid lines correspond to the two generation RH neutrino scenario where both $N_{1,2}$ can be produced on-shell from parent meson decay. The subsequent decays of $N_{1,2}$ lead to the same final state $e^+\mu^+\pi^-$ with

the same value of the branching ratio ². We have set the mixing angle, and phase as $\theta = \pi/4, \phi = \pi/2 + 0.1$ for blue dashed line. The solid blue line corresponds to the two generation scenario, with $\theta = \pi/4, \phi = 0.1$, and again corresponds the experimental limit on the branching ratio ³. We also show the effect of the interference on the future sensitivity. The black dashed line and black solid line correspond to a value of 10^{-12} for branching ratios of $K^+ \rightarrow e^+\mu^+\pi^-$, and $K^+ \rightarrow e^+e^+\pi^-$ which should be accessible after the full run of the NA62 experiment. In the right panel, we show the future sensitivity for B meson decays $B^+ \rightarrow e^+e^+\pi^-/e^+\mu^+\pi^-$. The two kinks occur, as new decay modes of the RH neutrinos into a lepton associated with a ρ and D meson open up in these mass ranges. The solid pink line in the right panel has been again derived by assuming only one generation RH neutrino state N_1 , where as blue dotted and red dashed lines stand for two generation RH neutrino scenario. For B meson case, we have considered the future sensitivity on the branching ratio to be $\mathcal{O}(10^{-12})$, which might be accessible in Belle-II or FCC-ee [19] ⁴. Note that, the limit on W_R can be significantly lowered in the presence of destructive interference as it leads to a natural suppression of the LNV branching ratio. Therefore, non-observation of any LNV signal for LRSM could signify the interference effects due to more than one generation of RH neutrinos.

V. RESULT FOR TWO GENERATION WITH THE FULL 3×3 MIXING MATRIX K_R

In the previous section, we considered a simple form of the K_R matrix, which contains only one angle and one phase. In general the mixing matrix K_R is a 3×3 unitary matrix, with more number of parameters. We consider a special scenario, where the K_R matrix is identical with the PMNS mixing matrix in the light neutrino

² Note that, the figures demonstrate the effect of interference in RH neutrino and RH gauge boson mass plane, without taking into account the probability of the RH neutrino to decay inside the detector. See [21] for further details, where the limits on M_N and M_{W_R} have been derived after taking into account the probability factor. In this work, we ignore the probability factor, as the main focus of the paper is to explore the interference effect in detail. This is to note that, a narrow mass range $0.20 \text{ GeV} < M_N < 0.45 \text{ GeV}$ of the right panel will also be accessible via K^+ meson decay.

³ We have not considered ϕ to be exactly $\pi/2$ or 0 as the theoretical branching ratio will be exactly zero and hence it is not possible to derive any kind of bound in $M_N - M_{W_R}$ plane.

⁴ The current bounds for the B meson LNV semileptonic decays are: $\text{BR}(B^+ \rightarrow e^+e^+\pi^-) \leq 2.3 \times 10^{-8}$ and $\text{BR}(B^+ \rightarrow e^+\mu^+\pi^-) \leq 1.5 \times 10^{-7}$ [37].

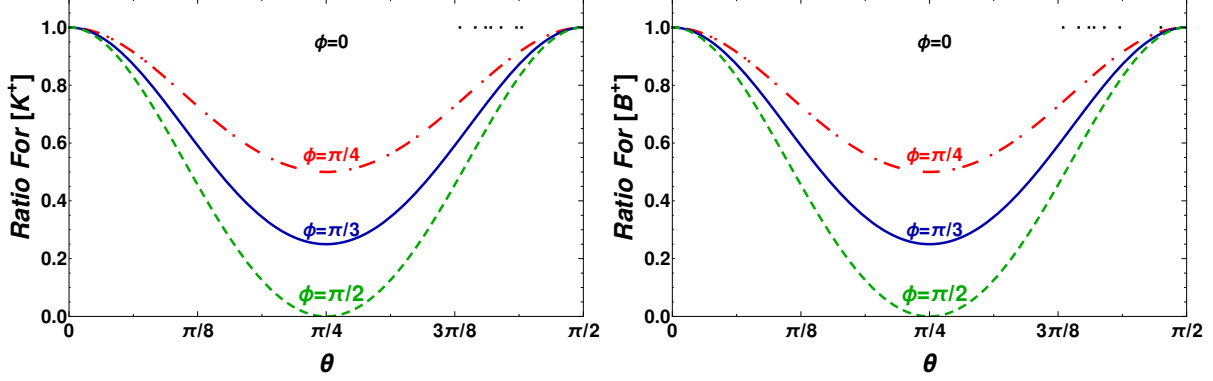


FIG. 8. Variation of the ratio of LNV and LNC decay to same flavour final state leptons (e^+, e^+ , and e^+, e^-) with the variation of the mixing angle θ . The left panel is for K^+ and right panel is for B^+ decay. The deviation of the ratio from identity occurs due to the interference between $N_{1,2}$ contributions.

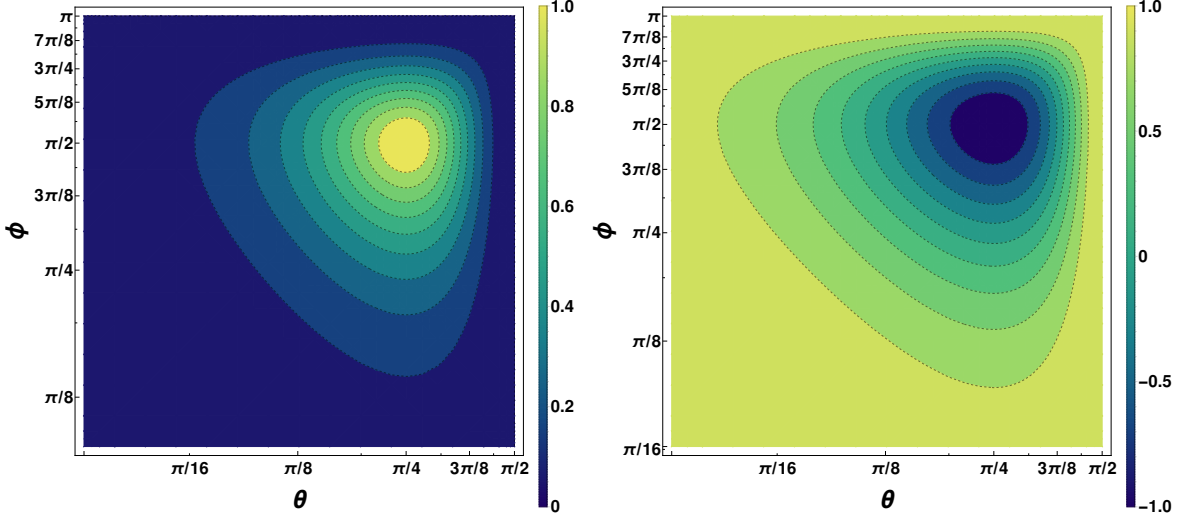


FIG. 9. Variation of R (left panel) and \tilde{R} (right panel) with the variation of angle and phase (θ, ϕ). R and \tilde{R} varies between $[0 : 1]$ and $[-1 : 1]$, respectively.

sector. The additional CP phases can give sizeable con-

tributions in the LNV meson decays. We have considered the following parameterisation of K_R ,

$$K_R = \begin{bmatrix} c_{12}c_{13}e^{i\alpha_1} & s_{12}c_{13}e^{i\alpha_1} & s_{13}e^{-i\delta}e^{i\alpha_1} \\ -s_{12}c_{23}e^{i\alpha_2} - c_{12}s_{23}s_{13}e^{i\delta}e^{i\alpha_2} & c_{12}c_{23}e^{i\alpha_2} - s_{12}s_{23}s_{13}e^{i\alpha_2}e^{i\delta} & s_{23}c_{13}e^{i\alpha_2} \\ s_{12}s_{23} - c_{12}c_{23}s_{13}e^{i\delta} & -c_{12}s_{23} - s_{12}c_{23}s_{13}e^{i\delta} & c_{23}c_{13} \end{bmatrix} \quad (46)$$

where s_{12}, s_{13}, s_{23} refer to $\sin \theta_{12}, \sin \theta_{13}, \sin \theta_{23}$, respectively, and $(\alpha_1, \alpha_2, \delta) \in (0, 2\pi)$. Considering such a 3×3 matrix the number of parameters increase and the result

is much more complicated as compared to the previous case. Note that, from Eq. 46, one would obtain Eq. 32, by considering $\theta_{13}, \theta_{23} = 0, \alpha_1 = 0$ and $\alpha_2 = \alpha$. In

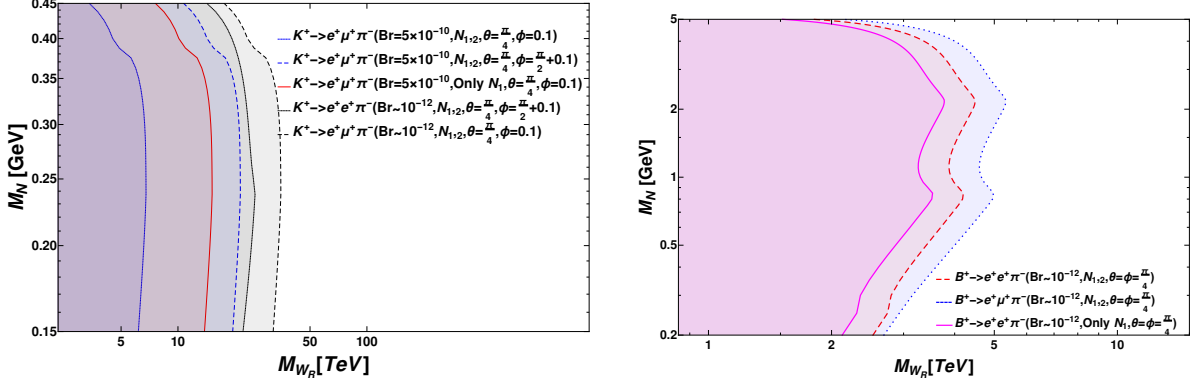


FIG. 10. Sensitivity of the RH neutrino mass M_N and the RH gauge boson mass M_{W_R} from the LNV processes $K^+ \rightarrow e^+e^+\pi^-$, $K^+ \rightarrow e^+\mu^+\pi^-$ (left panel) and $B^+ \rightarrow e^+\mu^+\pi^-$, $e^+e^+\pi^-$ (right panel). For K^+ decay mode in the left panel, the red solid line corresponds to one generation scenario, blue dashed line represents two generation scenario with constructive interference $\theta = \pi/4$, $\phi \sim 0, \pi/2$. The blue solid line represents two generation scenario with destructive interference. The black solid and dashed lines represent $Br \sim 10^{-12}$, which represents the sensitivity of future experiments. The figure in the right panel indicates the future sensitivity of LNV B^+ meson decay with $Br \sim 10^{-12}$.

Fig. 11, we show the variation of the LNV and LNC branching ratio $K^+ \rightarrow e^+e^+\pi^-$ and $K^+ \rightarrow e^+e^-\pi^+$ with the variation of the Dirac CP phase δ . We consider best fit values of the mixing angles $\theta_{12}, \theta_{13}, \theta_{23}$ for inverted mass hierarchy [38], and vary the Majorana phases $\alpha_{1,2}$ in between $0 - 2\pi$. The red region represents the LNV branching ratio, while the blue line corresponds to the LNC branching ratio. We also show the regions of δ , disallowed by the T2K neutrino oscillation experiment for inverted mass hierarchy. As can be seen, the LNV branching ratio varies with the variation of δ , as well as $\alpha_{1,2}$. The LNC mode is independent of Majorana phases $\alpha_{1,2}$. A deviation of the ratio of LNV and LNC branching ratio from unity occurs due to the simultaneous contributions of $N_{1,2}$ states in LNV and LNC processes, and possible interference effect.

VI. CONCLUSION

The LRSM is one of the most appealing models, that accommodate the embedding of RH neutrinos in a natural way. The model contains RH neutrinos, RH gauge bosons, and other BSM states that can offer distinctive experimental signatures. In this work, we explore the LNV and LNC semi-leptonic meson decays, mediated by the RH neutrinos and RH gauge bosons, and quantify the effect of interference in these decays due to the presence of at least two quasi-degenerate RH neutrino states. The RH neutrinos of masses MeV- few GeV can give a resonance enhancement in these rates, leading to these processes within the sensitivity reach of ongoing and future experiments, such as Belle II,

LHCb, and the different variations of the FCC. We consider two specific decay modes of K^+ and B^+ meson to $K^+/B^+ \rightarrow e^+e^+\pi^-$, $e^+e^-\pi^+$ and $K^+/B^+ \rightarrow e^+\mu^+\pi^-$, and analyse the effect of interference in detail. We consider two RH neutrinos to be nearly degenerate in mass with their masses in the range $M_{N_1} \sim M_{N_2} \sim 380$ MeV, and $M_{N_1} \sim M_{N_2} \sim 2$ GeV, relevant for the LNV and LNC K^+ and B^+ meson decays. In case of a single generation of RH neutrino, the LNV and LNC decay rates are the same, leading to the ratio of LNV and LNC branching to be unity. We find that, in the presence of interference between the two RH neutrino contributions in the amplitude, the LNV and LNC decay rates can differ widely, which leads to the ratio to be different than unity.

We first consider a simplistic scenario, where two RH neutrinos contribute to meson decay, with a simple RH neutrino mixing matrix dependent upon only one angle θ and one phase ϕ . We show that the LNV branching ratio, in particular the interference term, depends on both the angle and phase. For LNC, the branching ratio only depends on the angle, however, is insensitive to the phase. Few comments are in order:

- The channels $K^+ \rightarrow e^+e^+\pi^-$ and $K^+ \rightarrow e^+\mu^+\pi^-$ offer a complimentary nature in their predicted branching ratios. This holds true for other meson decays as well.
- We find that overall, the LNV branching ratios $K^+/B^+ \rightarrow e^+e^+\pi^-$ have a large variation w.r.t the variation in θ and ϕ . The decay rates are highly suppressed due to destructive interference at $\phi \sim \pi/2$, and $\theta \sim \pi/4$. For both the processes,

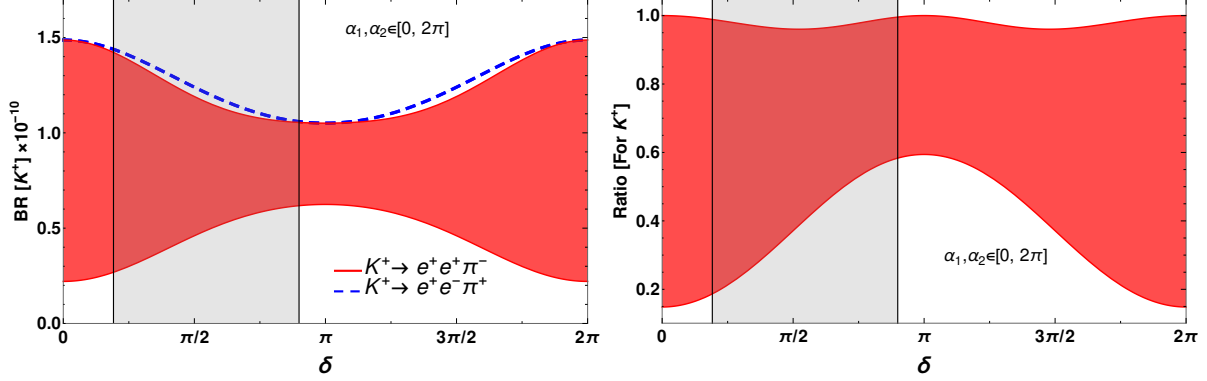


FIG. 11. Left panel: variation of the branching ratio of $K^+ \rightarrow e^+e^+\pi^-$, and $K^+ \rightarrow e^+e^-\pi^+$ decay modes, with the variation of the CP violating phase δ . The Majorana phases $\alpha_{1,2}$ have been varied in the denoted range. Right pane: variation of the ratio of LNV and LNC branching ratios with the variation of the CP phase δ . The shaded region is disallowed from the recent results from T2K. Note that, excluded region from T2K for δ is given with the convention $[-\pi : \pi]$, which we translated in the range $[0 : 2\pi]$ to be consistent with our convention. See text for more details.

the predicted branching ratios can reach maximum $\mathcal{O}(10^{-10}), \mathcal{O}(10^{-12})$ range with a RH gauge boson mass 22 TeV and 5 TeV, respectively. The predicted branching ratios falls within the sensitivity reach of the future experiments. The LNC branching ratio $K^+/B^+ \rightarrow e^+e^-\pi^+$ has a much less variation w.r.t the angle, while the rates are independent of the phase ϕ . Therefore, measurement in the LNC mode will not be able to provide any information about the CP-phase ϕ .

- For the different lepton flavor in the final states, $K^+ \rightarrow e^+\mu^-\pi^+$ mode, the LNC branching ratio is highly suppressed $\text{Br} \sim 10^{-15}$ (for B^+ mode, this is zero). This is beyond the sensitivity reach of the future experiments. However, the LNV branching ratio for $e^+\mu^+$ mode can offer a much larger branching ratio $\mathcal{O}(10^{-10})$ (for K^+ decay).

We also explore a scenario where the mixing matrix in the RH neutrino sector has the same form as the PMNS mixing in the neutrino sector. We consider

the best fit values of neutrino mixing parameters, and vary the phases. We find that, the Majorana phases in this case can have a large effect in the LNV branching ratio $K^+ \rightarrow e^+e^+\pi^-$, while the the LNC decay is independent of the Majorana phases. The ratio between LNV and LNC decays can again accommodate a large variation in the range $\mathcal{R} \sim (0.2 - 1)$. Any future measurement of the ratio, that is different than unity will indicate the presence of nearly degenerate RH neutrino states in LRSM.

ACKNOWLEDGMENTS

SM acknowledges the support from Spanish grant FPA2017-85216-P (AEI/FEDER, UE), PROMETEO/2018/165 (Generalitat Valenciana) and the Spanish Red Consolider MultiDark FPA2017-90566-REDC. MM and RG thank the *Indo-French Centre for the Promotion of Advanced Research* for the support (project no: 6304-2).

Appendix A: Details of LNV and LNC calculations

1. LNV

Amplitude from N_a contribution:

$$\mathcal{M}_{ij}^{\text{LNV},a} = 2G_F^2 V_{M_1}^{\text{CKM}} V_{M_2}^{\text{CKM}} f_{M_1} f_{M_2} \left(\frac{M_{WL}}{M_{WR}}\right)^4 (K_R^*)_{ai} (K_R^*)_{aj} M_{N_a} \frac{\bar{u}(k_1) \not{p} \not{k}_3 P_R v(k_2)}{q^2 - M_{N_a}^2 + i\Gamma_{N_a} M_{N_a}}, \quad (\text{A1})$$

Amplitude for leptonic exchange diagram:

$$\mathcal{M}_{ji}^{\text{LNV},a} = 2G_F^2 V_{M_1}^{\text{CKM}} V_{M_2}^{\text{CKM}} f_{M_1} f_{M_2} \left(\frac{M_{WL}}{M_{WR}} \right)^4 (K_R^*)_{aj} (K_R^*)_{ai} M_{N_a} \frac{\bar{u}(k_2) \not{p} \not{k}_3 P_R v(k_1)}{q^2 - M_{N_a}^2 + i\Gamma_{N_a} M_{N_a}}, \quad (\text{A2})$$

$$|\mathcal{M}_{ij}^{\text{LNV},a}|^2 = \kappa M_{N_a}^2 (K_R^*)_{ai} (K_R^*)_{aj} (K_R)_{ai} (K_R)_{aj} \frac{\text{Tr}[(\not{k}_2 - m_2) \not{k}_3 \not{p} P_L (\not{k}_1 + m_1) \not{p} \not{k}_3 P_R]}{(q^2 - M_{N_a}^2)^2 + \Gamma_{N_a}^2 M_{N_a}^2}, \quad (\text{A3})$$

$$|\mathcal{M}_{ji}^{\text{LNV},a}|^2 = \kappa M_{N_a}^2 (K_R^*)_{aj} (K_R^*)_{ai} (K_R)_{aj} (K_R)_{ai} \frac{\text{Tr}[(\not{k}_1 - m_1) \not{k}_3 \not{p} P_L (\not{k}_2 + m_2) \not{p} \not{k}_3 P_R]}{(q^2 - M_{N_a}^2)^2 + \Gamma_{N_a}^2 M_{N_a}^2}, \quad (\text{A4})$$

where $\kappa = 4G_F^4 (V_{M_1}^{\text{CKM}})^2 (V_{M_2}^{\text{CKM}})^2 f_{M_1}^2 f_{M_2}^2 \left(\frac{M_{WL}}{M_{WR}} \right)^8$. The interference terms are,

$$\begin{aligned} (\mathcal{M}_{ij}^{\text{LNV},a})^\dagger \mathcal{M}_{ij}^{\text{LNV},b} &= \kappa M_{N_a} M_{N_b} (K_R)_{ai} (K_R)_{aj} (K_R^*)_{bi} (K_R^*)_{bj} \\ &\times \frac{\text{Tr}[(\not{k}_2 - m_2) \not{k}_3 \not{p} P_L (\not{k}_1 + m_1) \not{p} \not{k}_3 P_R]}{(q^2 - M_{N_a}^2 - i\Gamma_{N_a} M_{N_a})(q^2 - M_{N_b}^2 + i\Gamma_{N_b} M_{N_b})} \end{aligned} \quad (\text{A5})$$

$$\begin{aligned} (\mathcal{M}_{ji}^{\text{LNV},a})^\dagger \mathcal{M}_{ji}^{\text{LNV},b} &= \kappa M_{N_a} M_{N_b} (K_R)_{aj} (K_R)_{ai} (K_R^*)_{bj} (K_R^*)_{bi} \\ &\times \frac{\text{Tr}[(\not{k}_1 - m_1) \not{k}_3 \not{p} P_L (\not{k}_2 + m_2) \not{p} \not{k}_3 P_R]}{(q^2 - M_{N_a}^2 - i\Gamma_{N_a} M_{N_a})(q^2 - M_{N_b}^2 + i\Gamma_{N_b} M_{N_b})} \end{aligned} \quad (\text{A6})$$

The traces are

$$\begin{aligned} \text{Tr}_{21} &= \text{Tr}[(\not{k}_2 - m_2) \not{k}_3 \not{p} P_L (\not{k}_1 + m_1) \not{p} \not{k}_3 P_R] = 2k_1 \cdot k_2 k_3 \cdot k_3 p \cdot p - 4k_1 \cdot p k_2 \cdot p k_3 \cdot k_3 \\ &\quad - 4k_1 \cdot k_3 k_2 \cdot k_3 p \cdot p + 8k_1 \cdot p k_2 \cdot k_3 k_3 \cdot p \end{aligned} \quad (\text{A7})$$

$$\begin{aligned} \text{Tr}_{12} &= \text{Tr}[(\not{k}_1 - m_1) \not{k}_3 \not{p} P_L (\not{k}_2 + m_2) \not{p} \not{k}_3 P_R] = 2k_1 \cdot k_2 k_3 \cdot k_3 p \cdot p - 4k_1 \cdot p k_2 \cdot p k_3 \cdot k_3 \\ &\quad - 4k_1 \cdot k_3 k_2 \cdot k_3 p \cdot p + 8k_1 \cdot k_3 k_2 \cdot p k_3 \cdot p \end{aligned} \quad (\text{A8})$$

As the RH neutrinos are produced onshell and having $\Gamma_{N_a} \ll M_{N_a}$, hence in our decay width calculation we can use narrow width approximation,

$$\frac{1}{(q^2 - M_{N_a}^2)^2 + \Gamma_{N_a}^2 M_{N_a}^2} \longrightarrow \frac{\pi}{\Gamma_{N_a} M_{N_a}} \delta(q^2 - M_{N_a}^2) \quad (\text{A9})$$

We can write the decay width as

$$\begin{aligned} d\Gamma^{\text{LNV}} &= \left(1 - \frac{\delta_{ij}}{2}\right) \frac{1}{2m} \frac{\kappa}{(2\pi)^5} \frac{\pi}{2} \frac{\pi}{4} d\cos\theta \times \\ &\left(\sum_a \left[M_{N_a}^2 K_{Rai} K_{Raj} K_{Rai}^* K_{Raj}^* \text{Tr}_{21} \lambda^{1/2} \left(1, \frac{m_i^2}{m^2}, \frac{M_{N_a}^2}{m^2}\right) \lambda^{1/2} \left(1, \frac{m_j^2}{M_{N_a}^2}, \frac{m_3^2}{M_{N_a}^2}\right) \frac{\pi}{\Gamma_{N_a} M_{N_a}} \right] + \right. \\ &\quad \sum_{a,b;b>a} \text{Re} \left[M_{N_a} M_{N_b} K_{Rai} K_{Raj} K_{Rbi}^* K_{Rbj}^* \text{Tr}_{21} \frac{\pi(\Gamma_{N_b} M_{N_b} + i(M_{N_a}^2 - M_{N_b}^2))}{(M_{N_a}^2 - M_{N_b}^2)^2 + \Gamma_{N_b}^2 M_{N_b}^2} \right] \\ &\quad \lambda^{1/2} \left(1, \frac{m_i^2}{m^2}, \frac{M_{N_a}^2}{m^2}\right) \lambda^{1/2} \left(1, \frac{m_j^2}{M_{N_a}^2}, \frac{m_3^2}{M_{N_a}^2}\right) + \sum_{a,b;b>a} \lambda^{1/2} \left(1, \frac{m_i^2}{m^2}, \frac{M_{N_b}^2}{m^2}\right) \lambda^{1/2} \left(1, \frac{m_j^2}{M_{N_b}^2}, \frac{m_3^2}{M_{N_b}^2}\right) \\ &\quad \left. \text{Re} \left[M_{N_a} M_{N_b} K_{Rai} K_{Raj} K_{Rbi}^* K_{Rbj}^* \text{Tr}_{21} \frac{\pi(\Gamma_{N_a} M_{N_a} - i(M_{N_b}^2 - M_{N_a}^2))}{(M_{N_b}^2 - M_{N_a}^2)^2 + \Gamma_{N_a}^2 M_{N_a}^2} \right] + (i \leftrightarrow j) \right) \quad (\text{A10}) \end{aligned}$$

LNC

Following the similar procedure the decay width for opposite sign leptons can be calculated as,

$$\mathcal{M}_{ij}^{\text{LNC},a} = 2G_F^2 V_{M_1}^{\text{CKM}} V_{M_2}^{\text{CKM}} f_{M_1} f_{M_2} \left(\frac{M_{W_L}}{M_{W_R}} \right)^4 (K_R)_{ai} (K_R^*)_{aj} \frac{\bar{u}(k_1) \not{p} \not{q} \not{k}'_3 P_R v(k_2)}{q^2 - M_{N_a}^2 + i\Gamma_{N_a} M_{N_a}} \quad (\text{A11})$$

$$|\mathcal{M}_{ij}^{\text{LNC},a}|^2 = \kappa (K_R^*)_{ai} (K_R)_{aj} (K_R)_{ai} (K_R^*)_{aj} \frac{\text{Tr} \left[(\not{k}'_2 - m_2) \not{k}'_3 \not{q} \not{p} P_R (\not{k}'_1 + m_1) \not{p} \not{q} \not{k}'_3 P_R \right]}{(q^2 - M_{N_a}^2)^2 + \Gamma_{N_a}^2 M_{N_a}^2} \quad (\text{A12})$$

where

$$\begin{aligned} \text{Tr}_{21}^{\text{LNC}} &= \text{Tr} \left[(\not{k}'_2 - m_2) \not{k}'_3 \not{q} \not{p} P_R (\not{k}'_1 + m_1) \not{p} \not{q} \not{k}'_3 P_R \right] = \\ &4k_1 \cdot q k_2 \cdot q k_3 \cdot k_3 p \cdot p - 8k_1 \cdot q k_2 \cdot k_3 k_3 \cdot q p \cdot p - 8k_1 \cdot p k_2 \cdot q k_3 \cdot k_3 p \cdot q + 16k_1 \cdot p k_2 \cdot k_3 k_3 \cdot q p \cdot q + \\ &4k_1 \cdot p k_2 \cdot p k_3 \cdot k_3 q \cdot q - 8k_1 \cdot p k_2 \cdot k_3 k_3 \cdot p q \cdot q + 4k_1 \cdot k_3 k_2 \cdot k_3 p \cdot p q \cdot q - 2k_1 \cdot k_2 k_3 \cdot k_3 p \cdot p q \cdot q \end{aligned} \quad (\text{A13})$$

We can write the LNC decay width as

$$\begin{aligned} d\Gamma^{\text{LNC}} &= \frac{1}{2m} \frac{\kappa}{(2\pi)^5} \frac{\pi}{2} \frac{\pi}{4} d\cos\theta \times \\ &\sum_a \left[K_{Rai} K_{Raj}^* K_{Rai}^* K_{Raj} \text{Tr}_{21}^{\text{LNC}} \lambda^{1/2} \left(1, \frac{m_i^2}{m^2}, \frac{M_{N_a}^2}{m^2} \right) \lambda^{1/2} \left(1, \frac{m_j^2}{M_{N_a}^2}, \frac{m_3^2}{M_{N_a}^2} \right) \frac{\pi}{\Gamma_{N_a} M_{N_a}} \right] + \\ &\sum_{a,b;b>a} \text{Re} \left[K_{Rai}^* K_{Raj} K_{Rbi} K_{Rbj}^* \text{Tr}_{21}^{\text{LNC}} \frac{\pi(\Gamma_{N_b} M_{N_b} + i(M_{N_a}^2 - M_{N_b}^2))}{(M_{N_a}^2 - M_{N_b}^2)^2 + \Gamma_{N_b}^2 M_{N_b}^2} \right] \\ &\lambda^{1/2} \left(1, \frac{m_i^2}{m^2}, \frac{M_{N_a}^2}{m^2} \right) \lambda^{1/2} \left(1, \frac{m_j^2}{M_{N_a}^2}, \frac{m_3^2}{M_{N_a}^2} \right) + \sum_{a,b;b>a} \lambda^{1/2} \left(1, \frac{m_i^2}{m^2}, \frac{M_{N_b}^2}{m^2} \right) \lambda^{1/2} \left(1, \frac{m_j^2}{M_{N_b}^2}, \frac{m_3^2}{M_{N_b}^2} \right) \\ &\text{Re} \left[K_{Rai}^* K_{Raj} K_{Rbi} K_{Rbj}^* \text{Tr}_{21}^{\text{LNC}} \frac{\pi(\Gamma_{N_a} M_{N_a} - i(M_{N_b}^2 - M_{N_a}^2))}{(M_{N_b}^2 - M_{N_a}^2)^2 + \Gamma_{N_a}^2 M_{N_a}^2} \right] \end{aligned} \quad (\text{A14})$$

Appendix B: Total decay width of heavy Majorana neutrino N_j

Here we give the computations of total decay width of N_j for our interested mass range $0.14 \text{ GeV} \leq M_{N_j} \leq 6 \text{ GeV}$. In addition to the SM gauge bosons W_L , Z , the gauge bosons W_R , Z' will also now contribute in the decays of RH neutrinos via charged current and neutral current interactions. The analytical expressions for different partial decay widths of the RH neutrinos N_i are given as

$$\begin{aligned} \Gamma(N_j \rightarrow \ell_i^- P^+) &= \frac{G_F^2 M_{N_j}^3}{16\pi} f_P^2 \left| V_{q\bar{q}'} \right|^2 \left(\left| S_{ij} \right|^2 F_P(x_{\ell_i}, x_P) + \left| K_{Rij} \right|^2 \xi_1^4 F_P(x_{\ell_i}, x_P) \right. \\ &\left. + 4\text{Re} [S_{ij} K_{Rij}] \xi_1^2 x_{\ell_i} x_P^2 \lambda^{\frac{1}{2}}(1, x_{\ell_i}^2, x_P^2) \right), \end{aligned}$$

where $\ell_1 = e, \ell_2 = \mu, \ell_3 = \tau$ and $P^+ = \pi^+, K^+, D^+, D_s^+$.

$$\begin{aligned} \Gamma(N_j \rightarrow \ell_i^- V^+) &= \frac{G_F^2 M_{N_j}^3}{16\pi} f_V^2 \left| V_{q\bar{q}'} \right|^2 \left(\left| S_{ij} \right|^2 F_V(x_{\ell_i}, x_V) + \left| K_{Rij} \right|^2 \xi_1^4 F_V(x_{\ell_i}, x_V) \right. \\ &\left. - 12\text{Re} [S_{ij} K_{Rij}] \xi_1^2 x_{\ell_i} x_V^2 \lambda^{\frac{1}{2}}(1, x_{\ell_i}^2, x_V^2) \right), \end{aligned}$$

where $\ell_1 = e, \ell_2 = \mu, \ell_3 = \tau$ and $V^+ = \rho^+, K^{*+}, D^{*+}, D_s^{*+}$.

$$\Gamma(N_j \rightarrow \nu_{\ell_i} P^0) = \frac{G_F^2 M_{N_j}^3}{4\pi} f_P^2 \sum_i |U_{ij}|^2 |S_{ij}|^2 \left(K_P^2 + K_P'^2 \xi_2^4 - 2K_P K_P' \xi_2^2 \right) F_P(x_{\nu_{\ell_i}}, x_P),$$

where ν_{ℓ_i} are the flavor eigenstates ν_e, ν_μ, ν_τ and $P^0 = \pi^0, \eta, \eta', \eta_c$.

$$\Gamma(N_j \rightarrow \nu_{\ell_i} V^0) = \frac{G_F^2 M_{N_j}^3}{4\pi} f_V^2 \sum_i |U_{ij}|^2 |S_{ij}|^2 \left(K_V^2 + K_V'^2 \xi_2^4 - 2K_V K_V' \xi_2^2 \right) F_V(x_{\nu_{\ell_i}}, x_P),$$

where $\nu_{\ell_i} = \nu_e, \nu_\mu, \nu_\tau$ and $V^0 = \rho^0, \omega, \phi, J/\psi$.

$$\Gamma(N_j \rightarrow \ell_i^- \ell_k^+ \nu_{\ell_k}) = \frac{G_F^2 M_{N_j}^5}{16\pi^3} \left(|S_{ij}|^2 \sum_{\kappa} |U_{k\kappa}|^2 I_1(x_{\ell_i}, x_{\nu_{\ell_k}}, x_{\ell_k}) + |K_{Rij}|^2 \sum_{\kappa} |T_{k\kappa}|^2 \xi_1^4 I_1(x_{\ell_i}, x_{\nu_{\ell_k}}, x_{\ell_k}) - 8Re(S_{ij}^* V_{ij}^* \sum_{\kappa} U_{k\kappa} T_{k\kappa}) \xi_1^2 I_3(x_{\ell_i}, x_{\nu_{\ell_k}}, x_{\ell_k}) \right),$$

where $\ell_i, \ell_j = e, \mu, \tau, \ell_i \neq \ell_j$.

$$\begin{aligned} \Gamma(N_j \rightarrow \nu_{\ell_i} \ell_i^- \ell_i^+) &= \frac{G_F^2 M_{N_j}^5}{16\pi^3} \left(|S_{ij}|^2 \sum_k |U_{ik}|^2 \left[I_1(x_{\nu_{\ell_i}}, x_{\ell_i}, x_{\ell_i}) + 2((g_V^\ell)^2 + (g_A^\ell)^2) \right. \right. \\ &I_1(x_{\nu_{\ell_i}}, x_{\ell_i}, x_{\ell_i}) + 2((g_V^\ell)^2 - (g_A^\ell)^2) I_2(x_{\nu_{\ell_i}}, x_{\ell_i}, x_{\ell_i}) + 2((g_V^{\prime\ell})^2 + (g_A^{\prime\ell})^2) \xi_2^4 I_1(x_{\nu_{\ell_i}}, x_{\ell_i}, x_{\ell_i}) \\ &+ 2((g_V^{\prime\ell})^2 - (g_A^{\prime\ell})^2) \xi_2^4 I_2(x_{\nu_{\ell_i}}, x_{\ell_i}, x_{\ell_i}) - 4\xi_2^2 ((g_V^\ell g_V^{\prime\ell} + g_A^\ell g_A^{\prime\ell}) I_1(x_{\nu_{\ell_i}}, x_{\ell_i}, x_{\ell_i}) \\ &\left. \left. + (g_V^\ell g_V^{\prime\ell} - g_A^\ell g_A^{\prime\ell}) I_2(x_{\nu_{\ell_i}}, x_{\ell_i}, x_{\ell_i}) \right] + |V_{ij}|^2 \sum_k |T_{ik}|^2 \xi_1^4 I_1(x_{\nu_{\ell_i}}, x_{\ell_i}, x_{\ell_i}) \right. \\ &- 8Re[S_{ij}^* V_{ij}^* \sum_k U_{ik} T_{ik}] \xi_1^2 I_3(x_{\ell_i}, x_{\nu_{\ell_i}}, x_{\ell_i}) + 2Re[|S_{ij}|^2 \sum_k |U_{ik}|^2] \left[\xi_2^2 (g_A^{\prime\ell} - g_V^{\prime\ell}) \right. \\ &I_1(x_{\nu_{\ell_i}}, x_{\ell_i}, x_{\ell_i}) - \xi_2^2 (g_A^\ell + g_V^\ell) I_2(x_{\nu_{\ell_i}}, x_{\ell_i}, x_{\ell_i}) - (g_A^\ell - g_V^\ell) I_1(x_{\nu_{\ell_i}}, x_{\ell_i}, x_{\ell_i}) + (g_A^\ell + g_V^\ell) \\ &I_2(x_{\nu_{\ell_i}}, x_{\ell_i}, x_{\ell_i}) \left. \right] - 8Re[S_{ij} V_{ij} \sum_k U_{ik}^* T_{ik}^*] \xi_1^2 \left[(g_V^{\prime\ell} - g_A^{\prime\ell}) \xi_2^2 I_3(x_{\nu_{\ell_i}}, x_{\ell_i}, x_{\ell_i}) + \frac{1}{4} (g_V^{\prime\ell} + g_A^{\prime\ell}) \xi_2^2 \right. \\ &\left. I_4(x_{\ell_i}, x_{\ell_i}, x_{\nu_{\ell_i}}) + (g_V^\ell - g_A^\ell) I_3(x_{\nu_{\ell_i}}, x_{\ell_i}, x_{\ell_i}) + \frac{1}{4} (g_V^\ell + g_A^\ell) I_4(x_{\ell_i}, x_{\ell_i}, x_{\nu_{\ell_i}}) \right] \Big), \end{aligned}$$

where $\ell_i = e, \mu, \tau$.

$$\begin{aligned} \Gamma(N_j \rightarrow \nu_{\ell_i} \ell_k^- \ell_k^+) &= \frac{G_F^2 M_{N_j}^5}{8\pi^3} |S_{ij}|^2 \sum_{\kappa} |U_{i\kappa}|^2 \left[((g_V^\ell)^2 + (g_A^\ell)^2) I_1(x_{\nu_{\ell_i}}, x_{\ell_k}, x_{\ell_k}) \right. \\ &+ ((g_V^\ell)^2 - (g_A^\ell)^2) I_2(x_{\nu_{\ell_i}}, x_{\ell_k}, x_{\ell_k}) + ((g_V^{\prime\ell})^2 + (g_A^{\prime\ell})^2) \xi_2^4 I_1(x_{\nu_{\ell_i}}, x_{\ell_k}, x_{\ell_k}) \\ &+ ((g_V^{\prime\ell})^2 - (g_A^{\prime\ell})^2) \xi_2^4 I_2(x_{\nu_{\ell_i}}, x_{\ell_k}, x_{\ell_k}) - 2\xi_2^2 [(g_V^\ell g_V^{\prime\ell} + g_A^\ell g_A^{\prime\ell}) I_1(x_{\nu_{\ell_i}}, x_{\ell_k}, x_{\ell_k}) \\ &\left. + (g_V^\ell g_V^{\prime\ell} - g_A^\ell g_A^{\prime\ell}) I_2(x_{\nu_{\ell_i}}, x_{\ell_k}, x_{\ell_k}) \right]. \end{aligned}$$

where $\ell_i, \ell_j = e, \mu, \tau$ and $\ell_i \neq \ell_j$.

$$\Gamma(N_j \rightarrow \nu_{\ell_i} \nu \bar{\nu}) = \frac{G_F^2 M_{N_j}^5}{192\pi^3} |S_{ij}|^2 \sum_k |U_{ik}|^2 \left(1 - \sin^2 \theta_w \xi_2^2 \right)^2,$$

where $\xi_1 = \frac{M_{W_L}}{M_{W_R}}$, $\xi_2 = \frac{M_Z}{M_{Z'}}$, $x_i = \frac{m_i}{M_N}$ with $m_i = m_\ell, m_{P^0}, m_{V^0}, m_{P^+}, m_V^+$. The kinematical function are given by,

$$\begin{aligned}
I_1(x, y, z) &= \int_{(x+y)^2}^{(1-z)^2} \frac{ds}{s} (s - x^2 - y^2)(1 + z^2 - s) \lambda^{\frac{1}{2}}(s, x^2, y^2) \lambda^{\frac{1}{2}}(1, s, z^2); \\
I_2(x, y, z) &= yz \int_{(y+z)^2}^{(1-x)^2} \frac{ds}{s} (1 + x^2 - s) \lambda^{\frac{1}{2}}(s, y^2, z^2) \lambda^{\frac{1}{2}}(1, s, x^2); \\
I_3(x, y, z) &= xyz \int_{(x+y)^2}^{(1-z)^2} \frac{ds}{s} \lambda^{\frac{1}{2}}(s, x^2, y^2) \lambda^{\frac{1}{2}}(1, s, z^2); \\
I_4(x, y, z) &= z \int_{(x+y)^2}^{(1-z)^2} \frac{ds}{s} \lambda^{\frac{1}{2}}(s, x^2, y^2) \lambda^{\frac{1}{2}}(1, s, z^2); \\
F_P(x, y) &= ((1 + x^2)(1 + x^2 - y^2) - 4x^2) \lambda^{\frac{1}{2}}(1, x^2, y^2); \\
F_V(x, y) &= ((1 - x^2)^2 + (1 + x^2)y^2 - 2y^4) \lambda^{\frac{1}{2}}(1, x^2, y^2).
\end{aligned}$$

Neutral current couplings of leptons are given by,

$$\begin{aligned}
g_V^\ell &= -\frac{1}{4} + \sin^2\theta_w, \quad g_A^\ell = \frac{1}{4}, \\
g_V^{\prime\ell} &= -\frac{1}{4} + \sin^2\theta_w, \quad g_A^{\prime\ell} = -\frac{1}{4} + \frac{1}{2}\sin^2\theta_w.
\end{aligned}$$

Neutral current coupling of pseudoscalar mesons are given by,

$$\begin{aligned}
K_{\pi^0} &= -\frac{1}{2\sqrt{2}}, \quad K'_{\pi^0} = \frac{1}{\sqrt{2}}(\frac{1}{2} - \sin^2\theta_w), \\
K_\eta &= -\frac{1}{2\sqrt{6}}, \quad K'_\eta = \frac{1}{\sqrt{6}}(\frac{1}{2} - \sin^2\theta_w), \\
K_{\eta'} &= \frac{1}{4\sqrt{3}}, \quad K'_{\eta'} = \frac{1}{\sqrt{3}}(-\frac{1}{4} + \frac{1}{2}\sin^2\theta_w), \\
K_{\eta_c} &= -\frac{1}{4}, \quad K'_{\eta_c} = (\frac{1}{4} - \frac{1}{2}\sin^2\theta_w),
\end{aligned}$$

Neutral current coupling of vector mesons are given by

$$\begin{aligned}
K_{\rho^0} &= \frac{1}{\sqrt{2}}(\frac{1}{2} - \sin^2\theta_w), \\
K_\omega &= -\frac{1}{3\sqrt{2}}\sin^2\theta_w, \\
K_\phi &= (-\frac{1}{4} + \frac{1}{3}\sin^2\theta_w), \\
K_{J/\psi} &= (\frac{1}{4} - \frac{2}{3}\sin^2\theta_w).
\end{aligned}$$

(B1)

The functions $A(M_N)$ and $B(M_N)$, relevant for $N \rightarrow l\pi$ decay mode is given by

$$A(M_N) = \frac{G_F^2 M_N^3}{16\pi} f_\pi^2 V_{ud}^2 \xi_1^4 \left[\frac{F_P(x_e, x_\pi) + F_P(x_\mu, x_\pi)}{2} \right] \quad (B2)$$

$$B(M_N) = \frac{G_F^2 M_N^3}{16\pi} f_\pi^2 V_{ud}^2 \xi_1^4 \left[\frac{F_P(x_e, x_\pi) - F_P(x_\mu, x_\pi)}{2} \right] \quad (B3)$$

[1] J. C. Pati and A. Salam, "Lepton Number as the Fourth Color," *Phys. Rev. D* **10** (1974) 275–289.

[Erratum: *Phys.Rev.D* 11, 703–703 (1975)].

- [2] GERDA Collaboration, M. Agostini *et al.*, “Improved Limit on Neutrinoless Double- β Decay of ^{76}Ge from GERDA Phase II,” *Phys. Rev. Lett.* **120** no. 13, (2018) 132503, [arXiv:1803.11100 \[nucl-ex\]](#).
- [3] G. Racah, “On the symmetry of particle and antiparticle,” *Nuovo Cim.* **14** (1937) 322–328.
- [4] W. Furry, “On transition probabilities in double beta-disintegration,” *Phys. Rev.* **56** (1939) 1184–1193.
- [5] J. Schechter and J. Valle, “Neutrinoless Double beta Decay in $\text{SU}(2) \times \text{U}(1)$ Theories,” *Phys. Rev. D* **25** (1982) 2951.
- [6] V. Tello, M. Nemevsek, F. Nesti, G. Senjanovic, and F. Vissani, “Left-Right Symmetry: from LHC to Neutrinoless Double Beta Decay,” *Phys. Rev. Lett.* **106** (2011) 151801, [arXiv:1011.3522 \[hep-ph\]](#).
- [7] P. S. Bhupal Dev, S. Goswami, and M. Mitra, “TeV Scale Left-Right Symmetry and Large Mixing Effects in Neutrinoless Double Beta Decay,” *Phys. Rev. D* **91** no. 11, (2015) 113004, [arXiv:1405.1399 \[hep-ph\]](#).
- [8] W.-Y. Keung and G. Senjanovic, “Majorana Neutrinos and the Production of the Right-handed Charged Gauge Boson,” *Phys. Rev. Lett.* **50** (1983) 1427.
- [9] C.-Y. Chen, P. S. B. Dev, and R. Mohapatra, “Probing Heavy-Light Neutrino Mixing in Left-Right Seesaw Models at the LHC,” *Phys. Rev. D* **88** (2013) 033014, [arXiv:1306.2342 \[hep-ph\]](#).
- [10] M. Mitra, R. Ruiz, D. J. Scott, and M. Spannowsky, “Neutrino Jets from High-Mass W_R Gauge Bosons in TeV-Scale Left-Right Symmetric Models,” *Phys. Rev. D* **94** no. 9, (2016) 095016, [arXiv:1607.03504 \[hep-ph\]](#).
- [11] M. Nemevsek, F. Nesti, and G. Popara, “Keung-Senjanović process at the LHC: From lepton number violation to displaced vertices to invisible decays,” *Phys. Rev. D* **97** no. 11, (2018) 115018, [arXiv:1801.05813 \[hep-ph\]](#).
- [12] M. Nemevsek, F. Nesti, and J. C. Vasquez, “Majorana Higgses at colliders,” *JHEP* **04** (2017) 114, [arXiv:1612.06840 \[hep-ph\]](#).
- [13] S. Mandal, *Search for sterile neutrinos at colliders*. PhD thesis, HBNI, Mumbai, 2019.
- [14] A. Atre, T. Han, S. Pascoli, and B. Zhang, “The Search for Heavy Majorana Neutrinos,” *JHEP* **05** (2009) 030, [arXiv:0901.3589 \[hep-ph\]](#).
- [15] LHCb Collaboration, R. Aaij *et al.*, “Search for Majorana neutrinos in $B^- \rightarrow \pi^+ \mu^- \mu^-$ decays,” *Phys. Rev. Lett.* **112** no. 13, (2014) 131802, [arXiv:1401.5361 \[hep-ex\]](#).
- [16] G. Cvetic, C. Dib, S. K. Kang, and C. Kim, “Probing Majorana neutrinos in rare K and D, \bar{D}_s , B, B_c meson decays,” *Phys. Rev. D* **82** (2010) 053010, [arXiv:1005.4282 \[hep-ph\]](#).
- [17] G. Cvetic, C. Kim, S. Mendizabal, and J. Zamora-Saa, “Exploring CP-violation, via heavy neutrino oscillations, in rare B meson decays at Belle II,” [arXiv:2007.04115 \[hep-ph\]](#).
- [18] B. Shuve and M. E. Peskin, “Revision of the LHCb Limit on Majorana Neutrinos,” *Phys. Rev. D* **94** no. 11, (2016) 113007, [arXiv:1607.04258 \[hep-ph\]](#).
- [19] E. J. Chun, A. Das, S. Mandal, M. Mitra, and N. Sinha, “Sensitivity of Lepton Number Violating Meson Decays in Different Experiments,” *Phys. Rev. D* **100** no. 9, (2019) 095022, [arXiv:1908.09562 \[hep-ph\]](#).
- [20] S. Mandal and N. Sinha, “Favoured B_c Decay modes to search for a Majorana neutrino,” *Phys. Rev. D* **94** no. 3, (2016) 033001, [arXiv:1602.09112 \[hep-ph\]](#).
- [21] S. Mandal, M. Mitra, and N. Sinha, “Constraining the right-handed gauge boson mass from lepton number violating meson decays in a low scale left-right model,” *Phys. Rev. D* **96** no. 3, (2017) 035023, [arXiv:1705.01932 \[hep-ph\]](#).
- [22] D. Milanes, N. Quintero, and C. E. Vera, “Sensitivity to Majorana neutrinos in $\Delta L = 2$ decays of B_c meson at LHCb,” *Phys. Rev. D* **93** no. 9, (2016) 094026, [arXiv:1604.03177 \[hep-ph\]](#).
- [23] A. Abada, V. De Romeri, M. Lucente, A. M. Teixeira, and T. Toma, “Effective Majorana mass matrix from tau and pseudoscalar meson lepton number violating decays,” *JHEP* **02** (2018) 169, [arXiv:1712.03984 \[hep-ph\]](#).
- [24] J. C. Helo, S. Kovalenko, and I. Schmidt, “Sterile neutrinos in lepton number and lepton flavor violating decays,” *Nucl. Phys. B* **853** (2011) 80–104, [arXiv:1005.1607 \[hep-ph\]](#).
- [25] A. Abada, C. Hati, X. Marcano, and A. Teixeira, “Interference effects in LNV and LFV semileptonic decays: the Majorana hypothesis,” *JHEP* **09** (2019) 017, [arXiv:1904.05367 \[hep-ph\]](#).
- [26] CMS Collaboration, A. M. Sirunyan *et al.*, “Search for a heavy right-handed W boson and a heavy neutrino in events with two same-flavor leptons and two jets at $\sqrt{s} = 13$ TeV,” *JHEP* **05** (2018) 148, [arXiv:1803.11116 \[hep-ex\]](#).
- [27] ATLAS Collaboration, M. Aaboud *et al.*, “Search for a right-handed gauge boson decaying into a high-momentum heavy neutrino and a charged lepton in pp collisions with the ATLAS detector at $\sqrt{s} = 13$ TeV,” *Phys. Lett. B* **798** (2019) 134942, [arXiv:1904.12679 \[hep-ex\]](#).
- [28] M. Hirsch and Z. S. Wang, “Heavy neutral leptons at ANUBIS,” *Phys. Rev. D* **101** no. 5, (2020) 055034, [arXiv:2001.04750 \[hep-ph\]](#).
- [29] J. Gluza and T. Jeliński, “Heavy neutrinos and the $pp \rightarrow lljj$ CMS data,” *Phys. Lett. B* **748** (2015) 125–131, [arXiv:1504.05568 \[hep-ph\]](#).
- [30] A. Das, P. S. B. Dev, and R. N. Mohapatra, “Same Sign versus Opposite Sign Dileptons as a Probe of Low Scale Seesaw Mechanisms,” *Phys. Rev. D* **97** no. 1, (2018) 015018, [arXiv:1709.06553 \[hep-ph\]](#).
- [31] J. Gunion, R. Vega, and J. Wudka, “Higgs triplets in the standard model,” *Phys. Rev. D* **42** (1990) 1673–1691.
- [32] R. N. Mohapatra and D. P. Sidhu, “Gauge Theories of Weak Interactions with Left-Right Symmetry and the Structure of Neutral Currents,” *Phys. Rev.* **D16** (1977) 2843.
- [33] V. Tello, *Connections between the high and low energy*

violation of Lepton and Flavor numbers in the minimal left-right symmetric model.

- [34] A. Dolgov, S. Hansen, G. Raffelt, and D. Semikoz, “Heavy sterile neutrinos: Bounds from big bang nucleosynthesis and SN1987A,” *Nucl. Phys. B* **590** (2000) 562–574, [arXiv:hep-ph/0008138](#).
- [35] M. Kawasaki, K. Kohri, and T. Moroi, “Big-Bang nucleosynthesis and hadronic decay of long-lived massive particles,” *Phys. Rev. D* **71** (2005) 083502, [arXiv:astro-ph/0408426](#).
- [36] M. Kawasaki, K. Kohri, T. Moroi, and Y. Takaesu, “Revisiting Big-Bang Nucleosynthesis Constraints on Long-Lived Decaying Particles,” *Phys. Rev. D* **97** no. 2, (2018) 023502, [arXiv:1709.01211 \[hep-ph\]](#).
- [37] **Particle Data Group** Collaboration, M. Tanabashi *et al.*, “Review of Particle Physics,” *Phys. Rev. D* **98** no. 3, (2018) 030001.
- [38] P. de Salas, D. Forero, S. Gariazzo, P. Martinez-Mirav, O. Mena, C. Ternes, M. Trtola, and J. Valle, “2020 Global reassessment of the neutrino oscillation picture,” [arXiv:2006.11237 \[hep-ph\]](#).